
CHIMERIC DRUG DESIGN WITH A NONCHARGED CARRIER FOR MITOCHONDRIAL DELIVERY

Consuelo Ripoll,¹ Pilar Herrero-Foncubierta,^{1,2} Virginia Puente-Muñoz,^{1,a} M. Carmen Gonzalez-Garcia,¹ Delia Miguel,¹ Sandra Resa,² Jose M. Paredes,¹ Maria J. Ruedas-Rama,¹ Emilio Garcia-Fernandez,¹ Miguel Martin,^{3,b} Mar Roldan,³ Susana Rocha,⁴ Herlinde De Keersmaecker,⁴ Johan Hofkens,⁴ Juan M. Cuerva,² and Angel Orte^{1,*}

¹ Departamento de Fisicoquímica, Unidad de Excelencia de Química Aplicada a Biomedicina y Medioambiente, Facultad de Farmacia, Universidad de Granada, Campus Cartuja, 18071 Granada, Spain

² Departamento de Química Orgánica, Unidad de Excelencia de Química Aplicada a Biomedicina y Medioambiente, Facultad de Ciencias, Universidad de Granada, Campus Fuentenueva, 18071 Granada, Spain

³ GENYO, Pfizer-University of Granada-Junta de Andalucía Centre for Genomics and Oncological Research. Avda. Ilustración 114. PTS, 18016, Granada, Spain

⁴ Department of Chemistry, K. U. Leuven, Celestijnenlaan 200F, B-3001, Heverlee, Belgium

Present addresses: ^a Interdisciplinary Institute for Neuroscience, UMR 5297, Centre National de la Recherche Scientifique, F-33076 Bordeaux, France; and Interdisciplinary Institute for Neuroscience, University of Bordeaux, F-33076 Bordeaux, France. ^b Departamento de Bioquímica y Biología Molecular I, Facultad de Ciencias, Universidad de Granada, Campus Fuentenueva, 18071 Granada, Spain

* **Corresponding author:** A. Orte, e-mail: angelorti@ugr.es. Tel. (+34) 958243825

TABLE OF CONTENTS

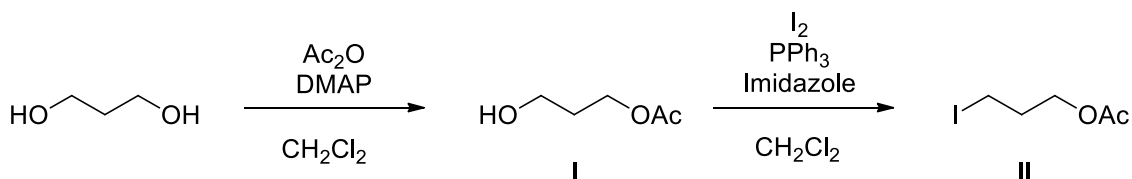
S1. Synthesis of the compounds in this work	3
S1.1. Synthesis of precursor reagents	3
S1.2. Synthesis of compound 1	3
S1.3. Synthesis of compound 2	4
S1.4. Synthesis of compound 3	6
S1.5. Synthesis of compound 4	6
S2. ¹H-NMR and ¹³C-NMR spectra of new compounds	7
S3. Supplementary Experimental Procedures	15
S3.1. Spectroscopy measurements	15

S3.2. Dual-color confocal fluorescence microscopy.....	15
S3.3. Dual-color fluorescence lifetime imaging microscopy (FLIM)	15
Table S1. Dual-color FLIM instrumental settings for colocalization studies of each dye.....	16
S3.4. Cell culture for fluorescence imaging	16
S3.5. Image analysis	17
S3.6. Cell viability assays	17
S.4. Supplementary spectroscopy figures of dyes 1-4	18
Figure S1. Absorption (A, C) and fluorescence emission (B, D) spectra of dyes 1 (A, B) and 4 (C, D) at different pH values.	18
Figure S2. Absorption and fluorescence emission dependence with pH of dyes 2 (A-C) and 3 (D-F) in aqueous solution.	19
S.5. Viscosity dependence of the fluorescence lifetime of dye 3	20
Figure S3. Average fluorescence lifetime, τ , of dye 3 in methanol:glycerine mixtures of different viscosity at 20, 30 and 40 °C.	20
S.7. Photostability of dyes 1-4.....	21
Figure S4. Photostability of dyes 1–4 during 2 h of continuous irradiation.....	21
S.7. Additional colocalization studies of dyes 1-4 with MT	22
Figure S5. Representative dual-color FLIM images of compound 1 in 143B cells and ρ_0 206 cells after 20 min of incubation with MT.....	22
Figure S6. Representative dual-color, super-resolution optical fluctuation imaging (SOFI) of 1 (green channel) and MT (red channel) in formaldehyde-fixed HeLa cells, and intensity plots of the profile lines.	23
Figure S7. Mitochondrial localization of compound 1 in 143B cells, after 20 min of incubation with MT, from dual-color FLIM images.	24
Figure S8. FLIM imaging of compound 1 in 143B cells.	25
Figure S9. Representative dual-color FLIM images of compound 2 in 143B (A, C, and E) and ρ_0 206 cells (B, D, and F), after 20 min of incubation with MT.....	26
Figure S10. Mitochondrial localization of compound 2 in ρ_0 206 cells, after 20 min of incubation with MT, from dual-color FLIM images.....	27
Figure S11. Mitochondrial localization of compound 3 in MDA-MB-231 cells, after 20 min of incubation with MT, from dual-color FLIM images.	28
Figure S12. FLIM imaging of compound 3 in MDA-MB-231 cells.....	29
Figure S13. Representative dual-color FLIM images of compound 4 in 143B (A, C, and E) and ρ_0 206 cells (B, D, and F), after 20 min of incubation with MT.....	30
Table S2. Pearson's correlation coefficient (PCC) and Manders' colocalization coefficient (MCC) values for the colocalization of dyes 1–4 with the mitochondria tracker MT. ^[a]	30
Figure S14. Representative dual-color fluorescence images of compound 1 (green) and the MT tracker (magenta) in 143B cells after 20 min of incubation with BAM15.	31
References	31

S1. SYNTHESIS OF THE COMPOUNDS IN THIS WORK

S1.1. SYNTHESIS OF PRECURSOR REAGENTS

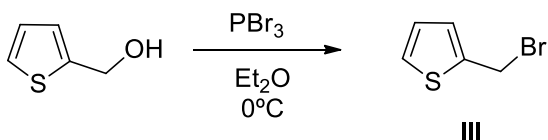
Synthesis of compound II



Compound I. To a solution of 1,3-propanediol (6.00 g, 0.08 mol) in CH_2Cl_2 (30 mL), DMAP (10.51 g, 0.09 mol) was added and subsequently acetic anhydride (8 mL, 0.09 mol) was added dropwise. The mixture was stirred for 2 h at room temperature. Silica gel was then added and the solvent was removed. The crude was purified by flash chromatography (SiO_2 , Hexane/EtOAc 6:4) to give compound I (4.01 g, 43%) as a colorless oil. ^1H and ^{13}C NMR spectra matched to those of the reported ones [1].

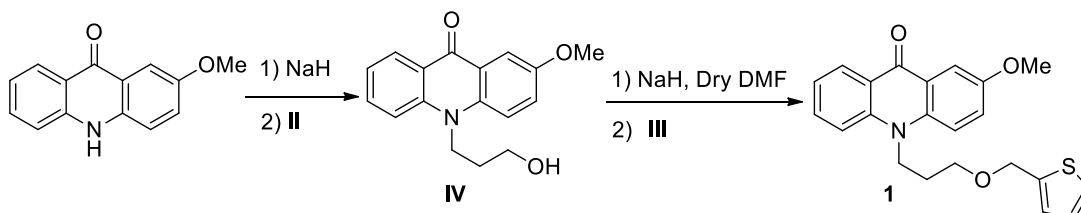
Compound II. To a solution of I_2 (12.92 g, 0.05 mol) in anhydrous CH_2Cl_2 (50 mL), triphenylphosphine (12.92 g, 0.05 mol) was added thus giving a brown-yellow solution. Then, imidazole (7.63 g, 0.11 mol) was added, changing the color to light yellow. Next, compound I (4.01 g, 0.03 mol) was added and the mixture was stirred at room temperature until consumption of the starting material (checked by TLC, around 1-2 h). Silica gel was then added and the solvent was removed. The crude was purified by flash chromatography (SiO_2 , Hexane/EtOAc 9:1) to give the compound II (6.43 g, 84%) as a yellow oil. ^1H NMR (500 MHz, CDCl_3) δ 4.13 (t, $J = 6.1$ Hz, 2H), 3.22 (t, $J = 6.8$ Hz, 2H), 2.14 (quint, $J = 6.6$ Hz, 2H), 2.06 (s, 3H). ^{13}C NMR (126 MHz, CDCl_3) δ 171.0 (C), 64.2 (CH_2), 32.5 (CH_2), 21.0 (CH_3), 1.5 (CH_2). HRMS (ESI): m/z $[\text{M}+\text{Na}]^+$ calcd for $\text{C}_5\text{H}_9\text{O}_2\text{I}\text{Na}$: 250.9539; found: 250.9535.

Synthesis of compound III



Compound III. To a solution of 2-thiophenemethanol (200 mg, 1.75 mmol) in anhydrous Et_2O at 0°C , PBr_3 (0.1 mL, 0.88 mmol) was added dropwise. The mixture was stirred for 30-45 minutes at room temperature and then quenched by addition of methanol, diluted with water and extracted with Et_2O . The organic layer was separated and dried with anhydrous Na_2SO_4 and the solvent was removed to give the compound III as a yellow liquid in quantitative yield. This compound was used in the next step without further purification. ^1H and ^{13}C NMR spectra matched to the reported ones [2].

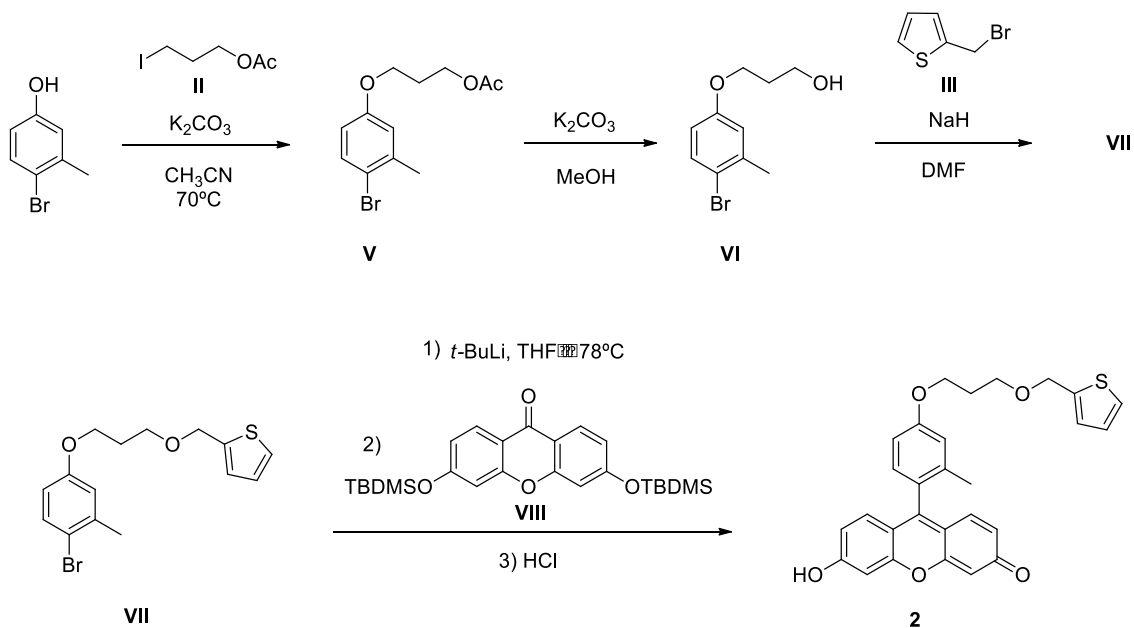
S1.2. SYNTHESIS OF COMPOUND 1



Compound IV. Compound **IV** was synthesized by the addition of 2-methoxyacridin-9(10H)-one to previously synthesized iodide **II** following a previously described procedure [3]. ^1H and ^{13}C NMR spectra matched to those of the reported one [4].

Compound 1. To a solution of **IV** (68 mg, 0.24 mmol) in anhydrous DMF (5 mL), NaH (60% in mineral oil, 30 mg, 0.72 mmol) was added. The resulting mixture was stirred for 10-15 minutes and then compound **III** (51 mg, 0.29 mmol) was added. The reaction mixture was stirred for another 24 h. After this time, the reaction was quenched by dropwise addition of water. The mixture was diluted with EtOAc and washed with HCl 10% (x3), the organic layer was separated and dried with anhydrous Na_2SO_4 and the solvent was removed. The residue was purified by flash chromatography (SiO_2 , Hexane/EtOAc 7:3) to give compound **1** (51 mg, 75%) as a yellow oil. An additional wash with hexane/dichloromethane mixtures gave compound **1** as yellow solid. ^1H NMR (500 MHz, MeOD) δ 8.41 (dd, $J = 8.1, 1.6$ Hz, 1H), 7.80 (d, $J = 3.2$ Hz, 1H), 7.78 – 7.71 (m, 3H), 7.41 (dd, $J = 5.1, 1.2$ Hz, 1H), 7.37 (dd, $J = 9.4, 3.1$ Hz, 1H), 7.28 (ddd, $J = 7.9, 6.4, 1.3$ Hz, 1H), 7.06 (dd, $J = 3.4, 1.1$ Hz, 1H), 7.01 (dd, $J = 5.1, 3.5$ Hz, 1H), 4.72 (s, 2H), 4.57 – 4.51 (m, 2H), 3.89 (s, 3H), 3.63 (t, $J = 5.5$ Hz, 2H), 2.15 – 2.07 (m, 2H). ^{13}C NMR (126 MHz, MeOD) δ 179.1 (C), 156.1 (C), 142.7 (C), 142.4 (C), 138.1 (C), 135.3 (CH), 128.1 (CH), 127.7 (CH), 127.5 (CH), 126.9 (CH), 126.2 (CH), 123.7 (C), 122.34 (CH), 122.28 (C), 118.6 (CH), 116.6 (CH), 106.9 (CH), 68.6 (CH_2), 67.9 (CH_2), 56.1 (CH_3), 44.4 (CH_2), 29.1 (CH_2). HRMS (ESI): m/z $[\text{M}+\text{Na}]^+$ calcd for $\text{C}_{22}\text{H}_{21}\text{NNaO}_3\text{S}$: 402.1140 found: 402.1123.

S1.3. SYNTHESIS OF COMPOUND 2



Compound V. To a solution of commercially available 4-bromo-3-methylphenol (300 mg, 1.60 mmol) in CH_3CN (10 mL) at 70 °C, K_2CO_3 (266 mg, 1.93 mmol) and compound **II** (439 mg, 1.93 mmol) were added. The reaction mixture was stirred at 70 °C for 24 h. Next, K_2CO_3 was filtrated, silica gel was added to the mixture and the solvent was removed. The residue was purified by flash chromatography (SiO_2 , Hexane/EtOAc 9:1) to give compound **V** (325 mg, 71%) as a light yellow liquid. ^1H NMR (400 MHz, CDCl_3) δ 7.39 (d, $J = 8.7$ Hz, 1H), 6.78 (d, $J = 3.0$ Hz, 1H), 6.60 (dd, $J = 8.7, 3.0$ Hz, 1H), 4.25 (t, $J = 6.3$ Hz, 2H), 4.00 (t, $J = 6.1$ Hz, 2H), 2.36 (s, 3H), 2.10 (quint, $J = 6.3$ Hz, 2H), 2.05 (s, 3H). ^{13}C NMR (101 MHz, CDCl_3) δ 171.2 (C), 158.1 (C), 139.0 (C), 133.0 (CH), 117.3 (CH), 115.7 (C), 113.6 (CH), 64.7 (CH_2), 61.3 (CH_2), 28.7

(CH₂), 23.3 (CH₃), 21.1 (CH₃). HRMS (ESI): *m/z* [M+Na]⁺ calcd for C₁₂H₁₅O₃BrNa: 309.0096 found: 309.0092.

Compound VI. To a solution of compound **V** (325 mg, 1.13 mmol) in MeOH (10 mL), K₂CO₃ (469 mg, 3.40 mmol) was added. The mixture was stirred at room temperature for 15 min. Silica gel was then added and the solvent was removed. The crude was purified by flash chromatography (SiO₂, Hexane/EtOAc 6:4) to give the compound **VI** (234 mg, 84%) as a light yellow liquid. ¹H NMR (400 MHz, CDCl₃) δ 7.39 (d, *J* = 8.7 Hz, 1H), 6.80 (d, *J* = 3.0 Hz, 1H), 6.62 (dd, *J* = 8.7, 3.0 Hz, 1H), 4.08 (t, *J* = 6.0 Hz, 2H), 3.85 (q, *J* = 5.5 Hz, 2H), 2.36 (s, 3H), 2.03 (quint, *J* = 6.0 Hz, 2H), 1.69 (t, *J* = 4.7 Hz, 1H). ¹³C NMR (101 MHz, CDCl₃) δ 158.1 (C), 139.0 (C), 133.0 (CH), 117.3 (CH), 115.7 (C), 113.6 (CH), 66.0 (CH₂), 60.5 (CH₂), 32.1 (CH₂), 23.3 (CH₃). HRMS (ESI): *m/z* [M+Na]⁺ calcd for C₁₀H₁₃O₂BrNa: 266.9991 found: 266.9980.

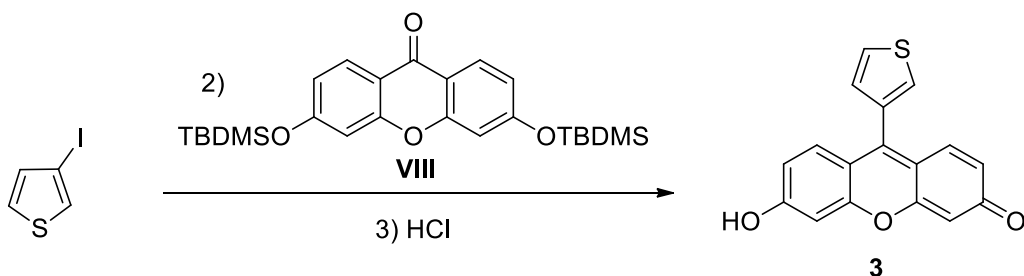
Compound VII. To a solution of compound **VI** (234 mg, 0.95 mmol) in anhydrous DMF (6 mL), NaH (60% in mineral oil, 115 mg, 2.87 mmol) and compound **III** (254 mg, 1.43 mmol) were added. The mixture was stirred at room temperature for 16 h. After this time, the mixture was quenched by dropwise addition of water, diluted with EtOAc and washed with HCl 10%. The organic layer was dried with anhydrous Na₂SO₄ and the solvent was removed. The residue was purified by flash chromatography (SiO₂, Hexane/EtOAc 98:2) to give compound **VII** (279 mg, 86%) as a light yellow liquid. ¹H NMR (400 MHz, CDCl₃) δ 7.38 (d, *J* = 8.7 Hz, 1H), 7.27 (dd, *J* = 4.9, 1.4 Hz, 1H), 7.00 – 6.98 (m, 1H), 6.96 (dd, *J* = 4.9, 3.5 Hz, 1H), 6.78 (d, *J* = 3.0 Hz, 1H), 6.60 (dd, *J* = 8.7, 3.0 Hz, 1H), 4.68 (s, 2H), 4.03 (t, *J* = 6.3 Hz, 2H), 3.65 (t, *J* = 6.1 Hz, 2H), 2.36 (s, 3H), 2.05 (quint, *J* = 6.2 Hz, 2H). ¹³C NMR (101 MHz, CDCl₃) δ 158.4 (C), 141.3 (C), 138.8 (C), 132.9 (CH), 126.8 (CH), 126.4 (CH), 125.9 (CH), 117.3 (CH), 115.5 (C), 113.7 (CH), 67.7 (CH₂), 66.5 (CH₂), 65.1 (CH₂), 29.8 (CH₂), 23.3 (CH₃). HRMS (ESI): *m/z* [M+Na]⁺ calcd for C₁₅H₁₇O₂SBrNa: 363.0024 found: 363.0028.

Compound VIII. Compound **VIII** was prepared according to a previously described procedure. ¹H and ¹³C NMR spectra matched to the reported ones [5].

Compound 2. To a solution of compound **VII** (279 mg, 0.82 mmol) in freshly distilled THF (4 mL) under an Ar atmosphere at –78 °C, *t*-BuLi (1.7 M in hexane, 0.96 mL, 1.64 mmol) was added dropwise. After keeping the reaction at that temperature for 20 minutes, a solution of compound **VIII** (187 mg, 0.41 mmol) in THF (2 mL) was slowly added. Then, the mixture was stirred at –78 °C for 15 minutes and then allowed to reach room temperature. The reaction was monitored by TLC. After consumption of compound **VIII**, HCl 10% (1 mL) was added promoting a color change from light yellow to orange. Finally, solvent was removed and residue was purified by flash chromatography (SiO₂, CH₂Cl₂/MeOH 9:1) to give compound **2** (130 mg, 66%) as an orange solid. ¹H NMR (400 MHz, MeOD) δ 7.36 (dd, *J* = 5.1, 1.2 Hz, 1H), 7.12 (d, *J* = 8.4 Hz, 1H), 7.08 (d, *J* = 9.7 Hz, 2H), 7.05 – 7.03 (m, 1H), 7.00 (d, *J* = 2.5 Hz, 1H), 6.99 – 6.94 (m, 2H), 6.68 – 6.64 (m, 4H), 4.72 (s, 2H), 4.17 (t, *J* = 6.2 Hz, 2H), 3.72 (t, *J* = 6.1 Hz, 2H), 2.09 (quint, *J* = 6.2 Hz, 2H), 2.02 (s, 3H). ¹³C NMR (101 MHz, MeOD) δ 179.0 (C), 161.5 (C), 159.7 (C), 156.5 (C), 142.5 (C), 138.9 (C), 132.3 (CH), 131.5 (CH), 127.59 (CH) 127.58 (CH), 126.8 (CH), 126.0 (C), 123.4 (CH), 117.6 (CH), 115.5 (C), 113.3 (CH), 104.5 (CH), 68.3 (CH₂), 67.4 (CH₂), 66.0 (CH₂), 30.7 (CH₂), 20.0 (CH₃). HRMS (ESI): *m/z* [M+H]⁺ calcd for C₂₈H₂₅O₅S: 473.1417 found: 473.1416.

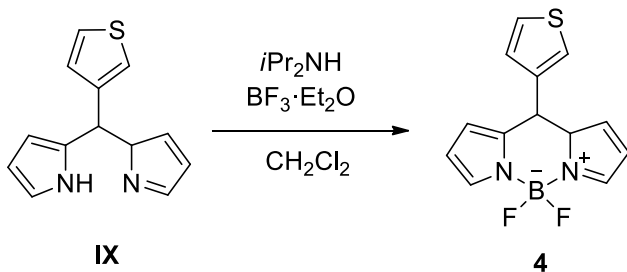
S1.4. SYNTHESIS OF COMPOUND 3

1) *t*-BuLi, THF, -50 °C



Compound 3. To a solution of 3-iodothiophene (118 mg, 0.56 mmol) in freshly distilled THF (2 mL) under Ar atmosphere at -50 °C, *t*-BuLi (1.7 M in hexane, 0.66 mL, 1.12 mmol) was added dropwise. After keeping the reaction at that temperature for 20 minutes, a solution of compound VIII (128 mg, 0.28 mmol) in THF (2 mL) was slowly added. Then, the mixture was stirred at -50 °C for 15 minutes and then allowed to reach room temperature. The reaction was monitored by TLC. After consumption of compound VIII, HCl 10% (1 mL) was added promoting a color change from light yellow to orange. Finally, solvent was removed and residue was purified by flash chromatography (SiO₂, CH₂Cl₂/MeOH 8:2) to give the compound 3 (48 mg, 59%) as an orange solid. ¹H NMR (500 MHz, DMSO-*d*₆) δ 7.93 – 7.87 (m, 2H), 7.32 (dd, *J* = 4.7, 1.4 Hz, 1H), 7.22 (d, *J* = 9.3 Hz, 2H), 6.64 (bs, 4H). ¹³C NMR (126 MHz, DMSO-*d*₆) δ 145.4 (C), 132.2 (C), 130.5 (CH), 129.3 (CH), 128.0 (CH), 127.7 (CH). Several carbons are not observed. HRMS (EI): *m/z* [M]⁺ calcd for C₁₇H₁₀O₃S: 294.0351 found: 294.0339.

S1.5. SYNTHESIS OF COMPOUND 4

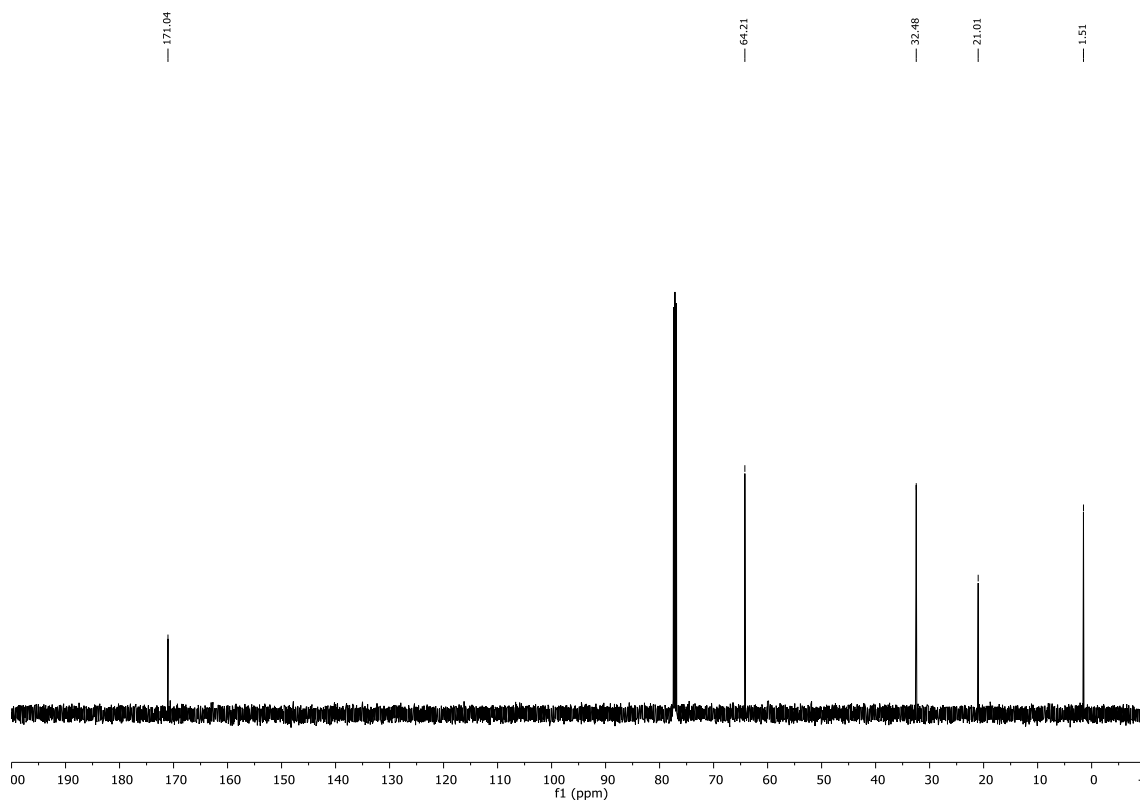
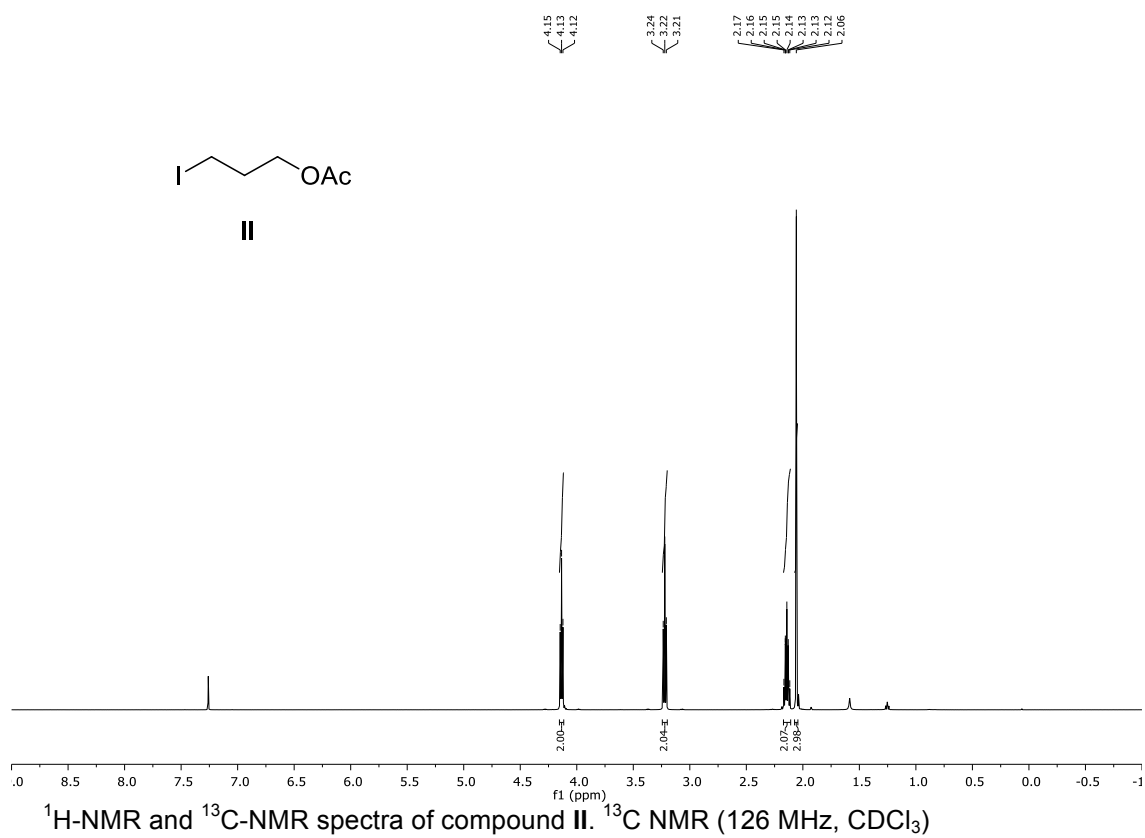


Compound IX. Compound IX was prepared according to a previously described procedure. ¹H and ¹³C NMR spectra matched those of the reported ones [6].

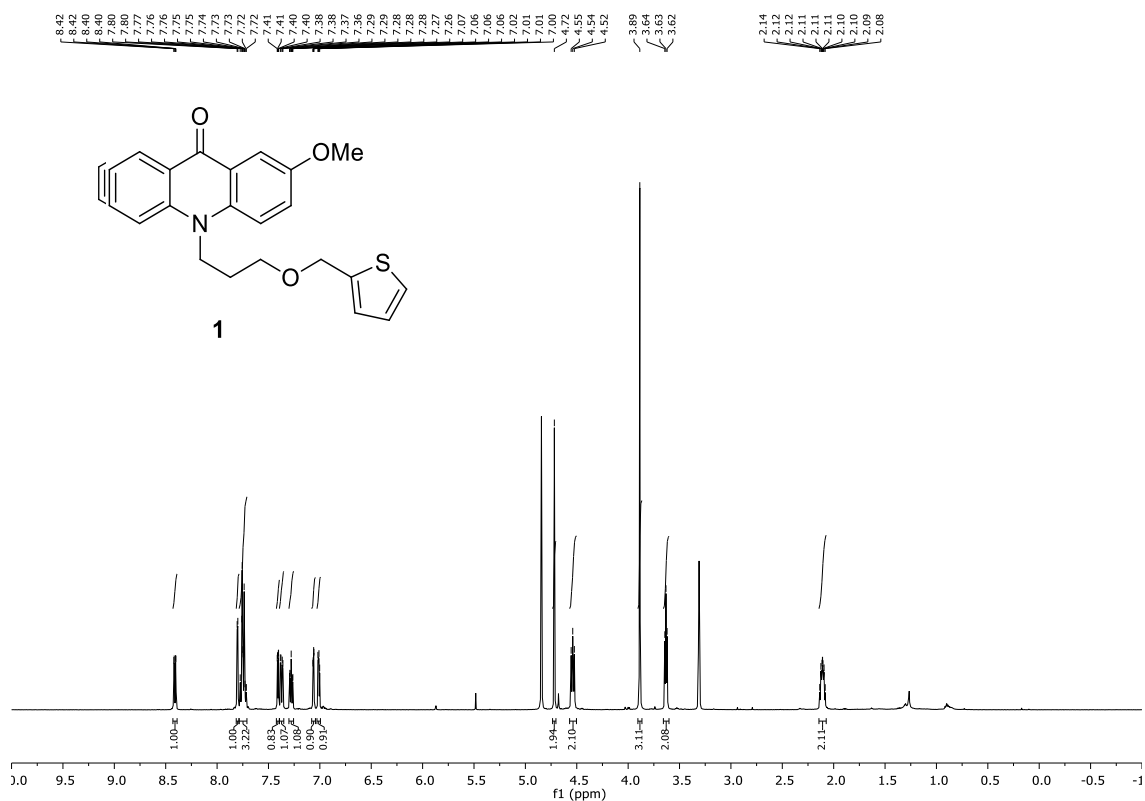
Compound 4. To a solution of compound IX (100 mg, 0.44 mmol) in CH₂Cl₂ (5 ml), diisopropylamine (0.3 ml, 2.12 mmol) was added. The mixture was stirred for 1 h at room temperature. Then BF₃·OEt₂ (0.55 ml, 2.12 mmol) was added and the resulting mixture was heated under reflux. The reaction was monitored by TLC until consumption of starting materials. The mixture was allowed to cool to room temperature, diluted with water and washed with CH₂Cl₂, the organic layer was separated and dried with anhydrous Na₂SO₄ and the solvent was removed. The residue was purified by flash chromatography (SiO₂, CH₂Cl₂/MeOH 9:1) to give the compound 4 (65 mg, 53%) as a yellow-brown solid. ¹H and ¹³C NMR spectra matched those of the reported ones [6].

S2. ^1H -NMR AND ^{13}C -NMR SPECTRA OF NEW COMPOUNDS

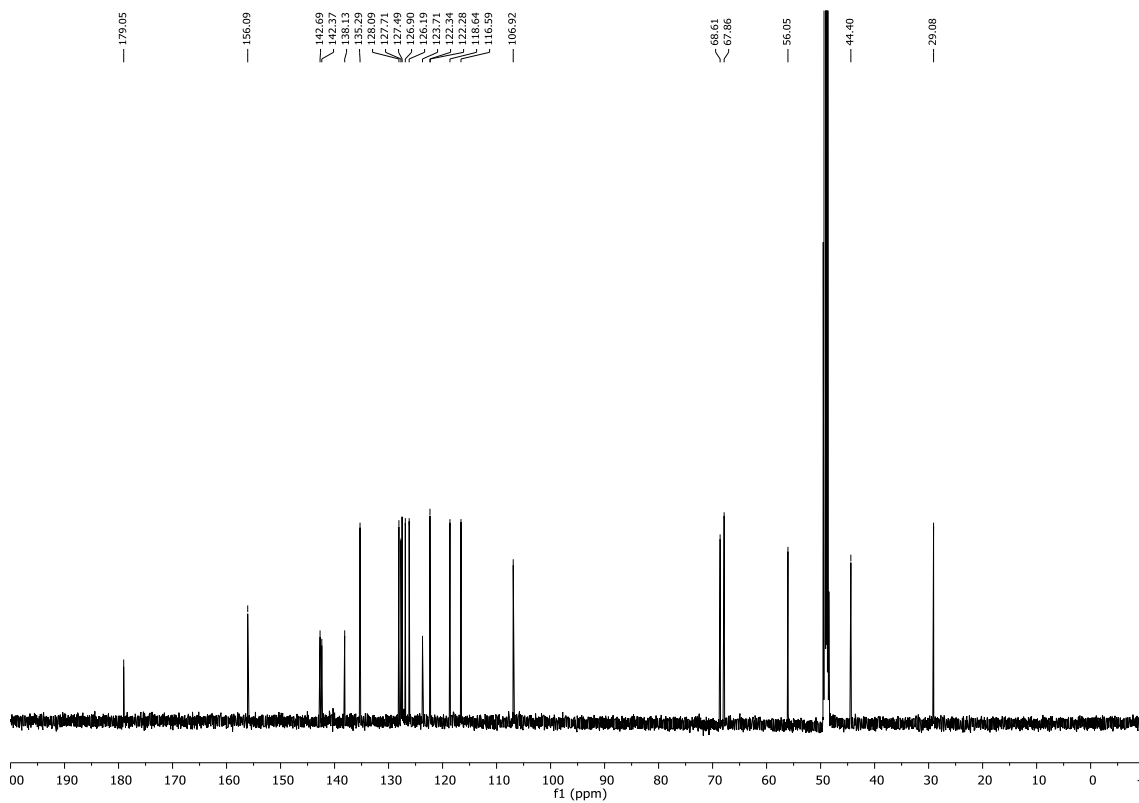
^1H -NMR and ^{13}C -NMR spectra of compound II. ^1H NMR (500 MHz, CDCl_3)



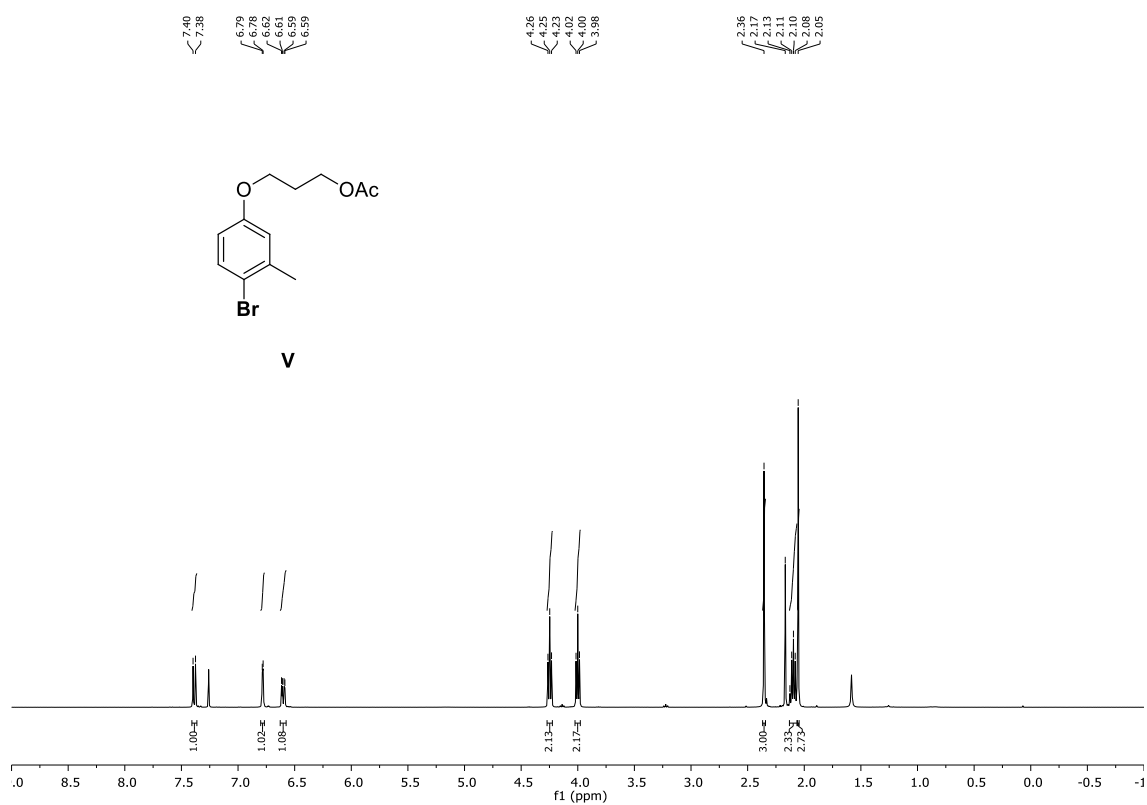
¹H-NMR and ¹³C-NMR spectra of compound 1. ¹H NMR (500 MHz, MeOD)



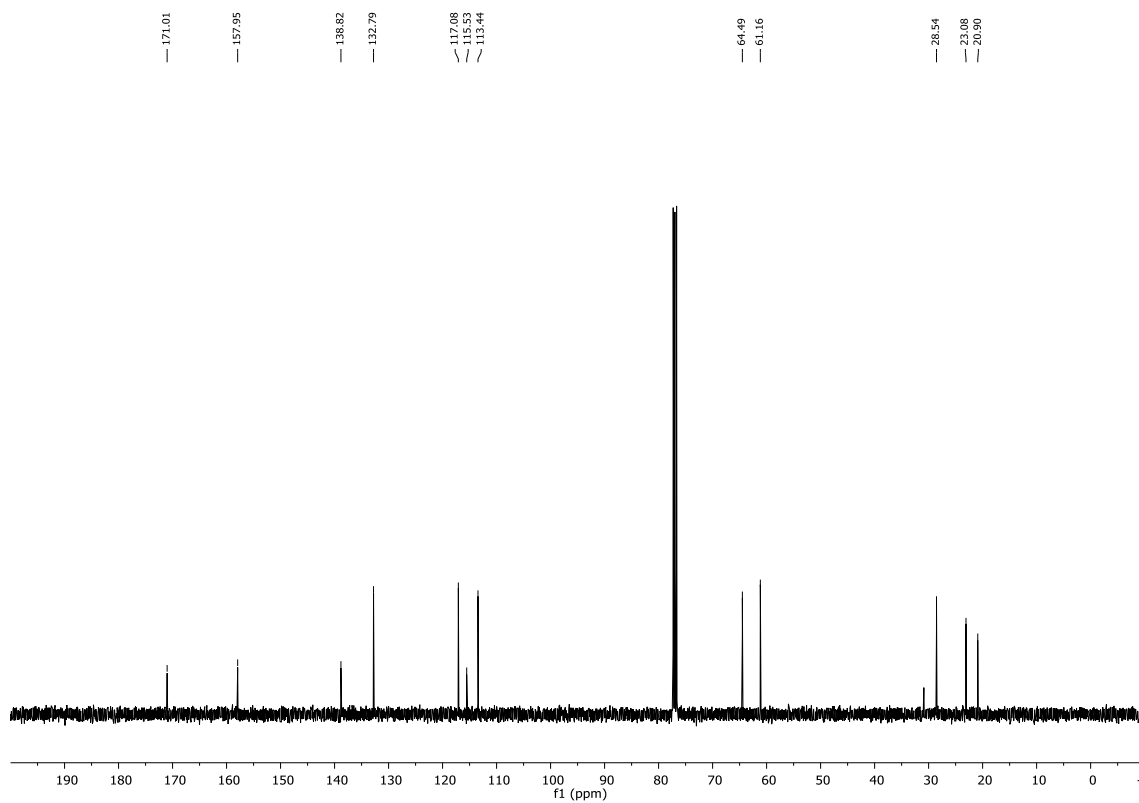
¹H-NMR and ¹³C-NMR spectra of compound 1. ¹³C NMR (126 MHz, MeOD)



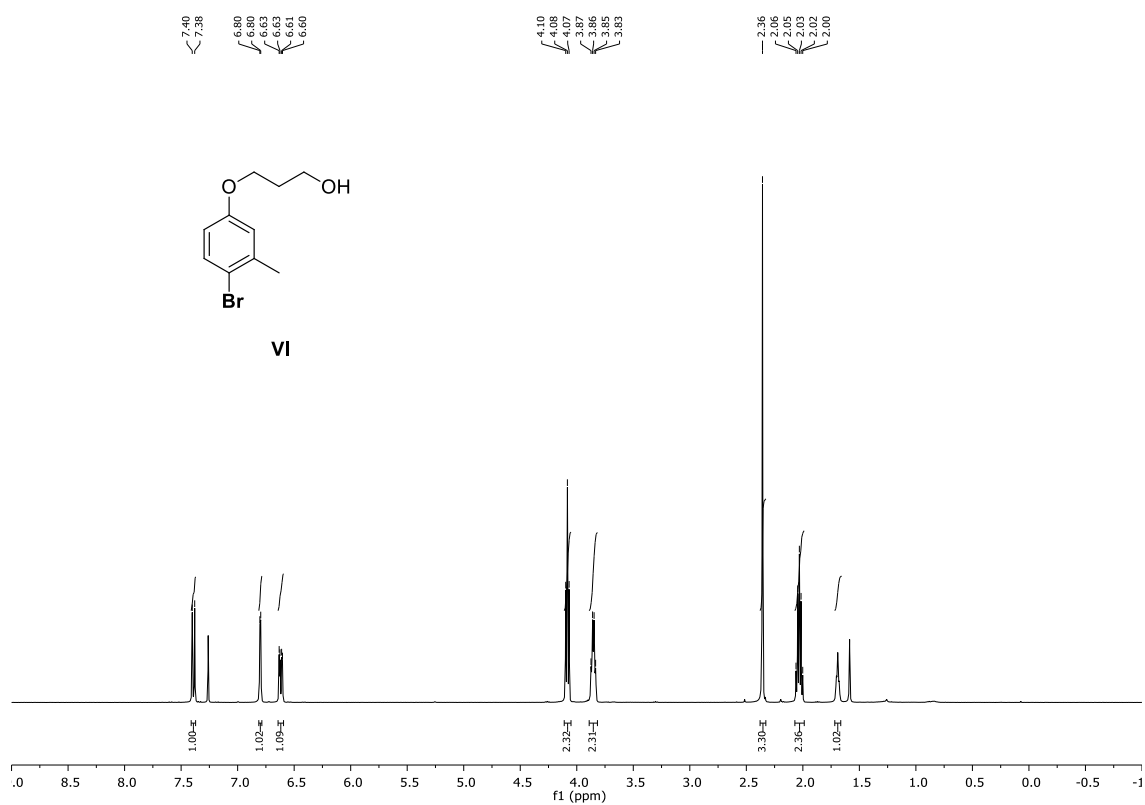
$^1\text{H-NMR}$ and $^{13}\text{C-NMR}$ spectra of compound **V**. $^1\text{H NMR}$ (400 MHz, CDCl_3)



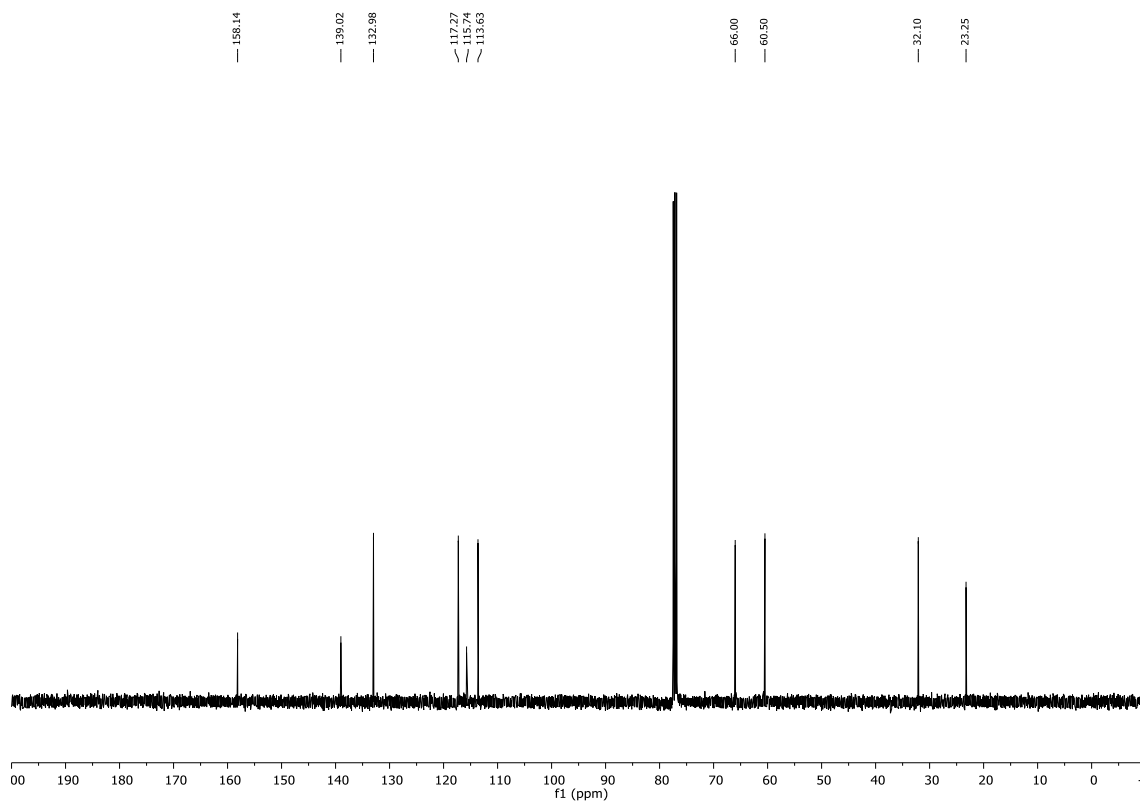
$^1\text{H-NMR}$ and $^{13}\text{C-NMR}$ spectra of compound **V**. $^{13}\text{C NMR}$ (101 MHz, CDCl_3)



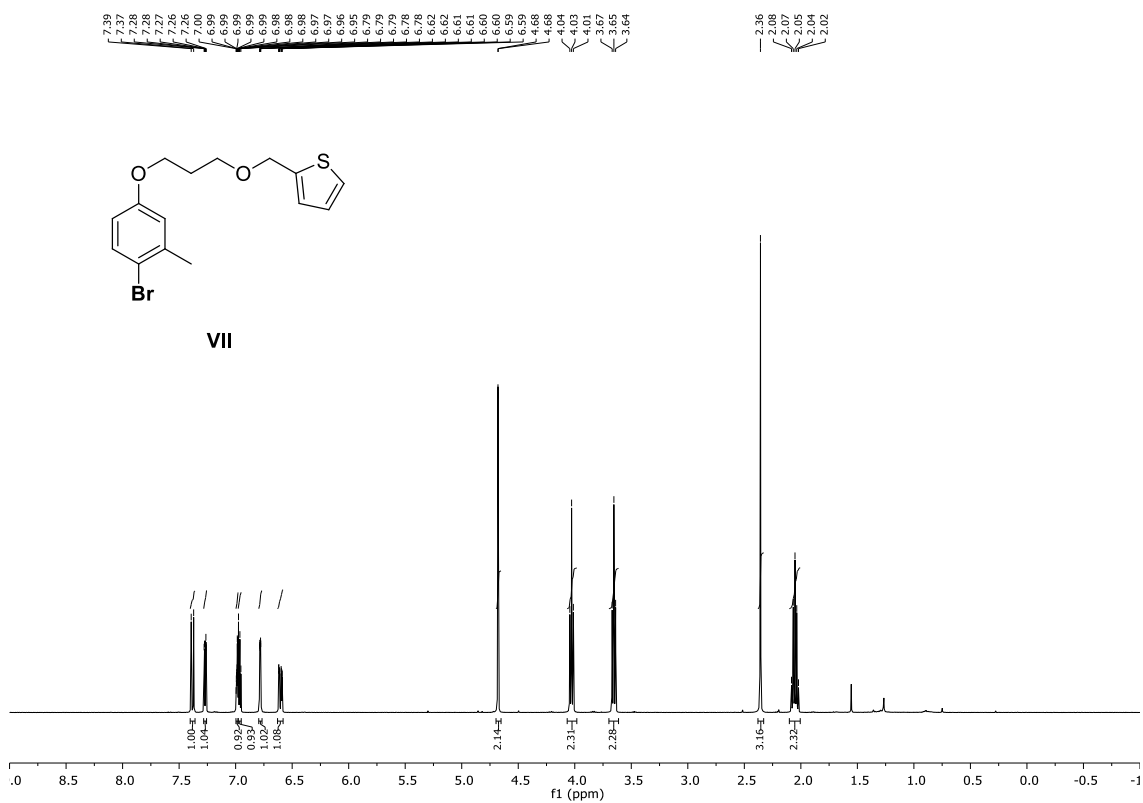
$^1\text{H-NMR}$ and $^{13}\text{C-NMR}$ spectra of compound **VI**. $^1\text{H NMR}$ (400 MHz, CDCl_3)



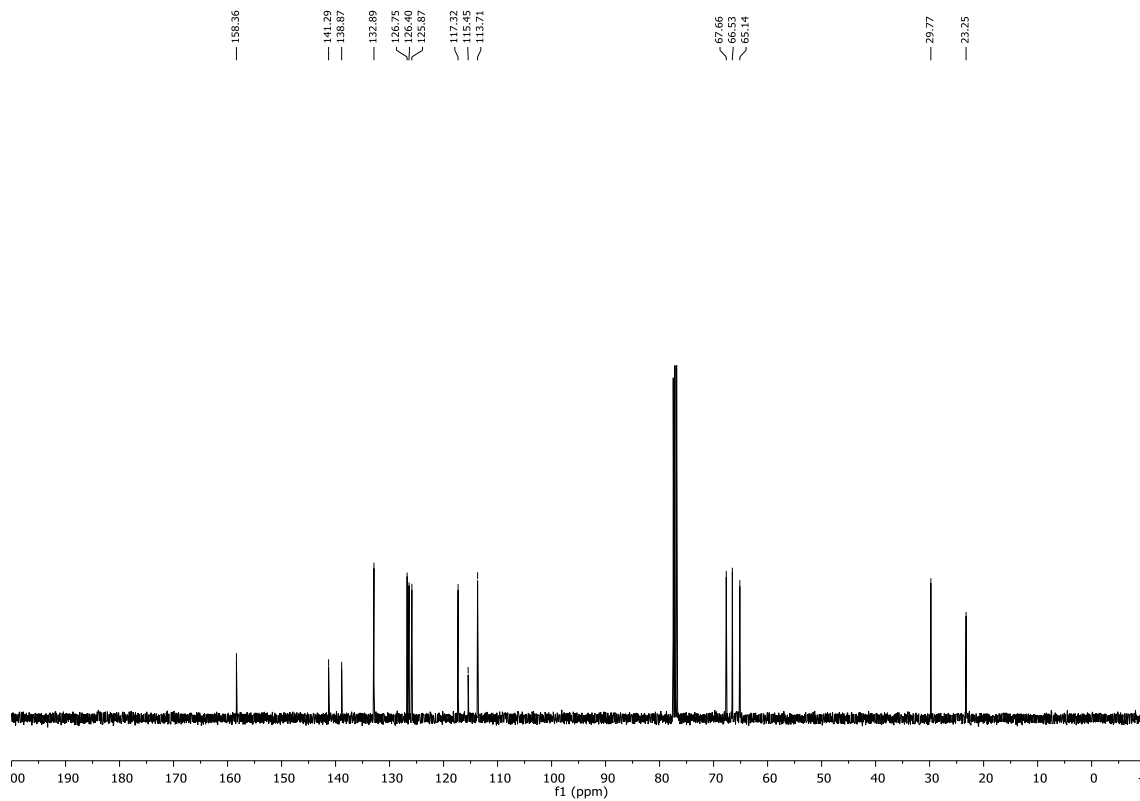
$^1\text{H-NMR}$ and $^{13}\text{C-NMR}$ spectra of compound **VI**. $^{13}\text{C NMR}$ (101 MHz, CDCl_3)



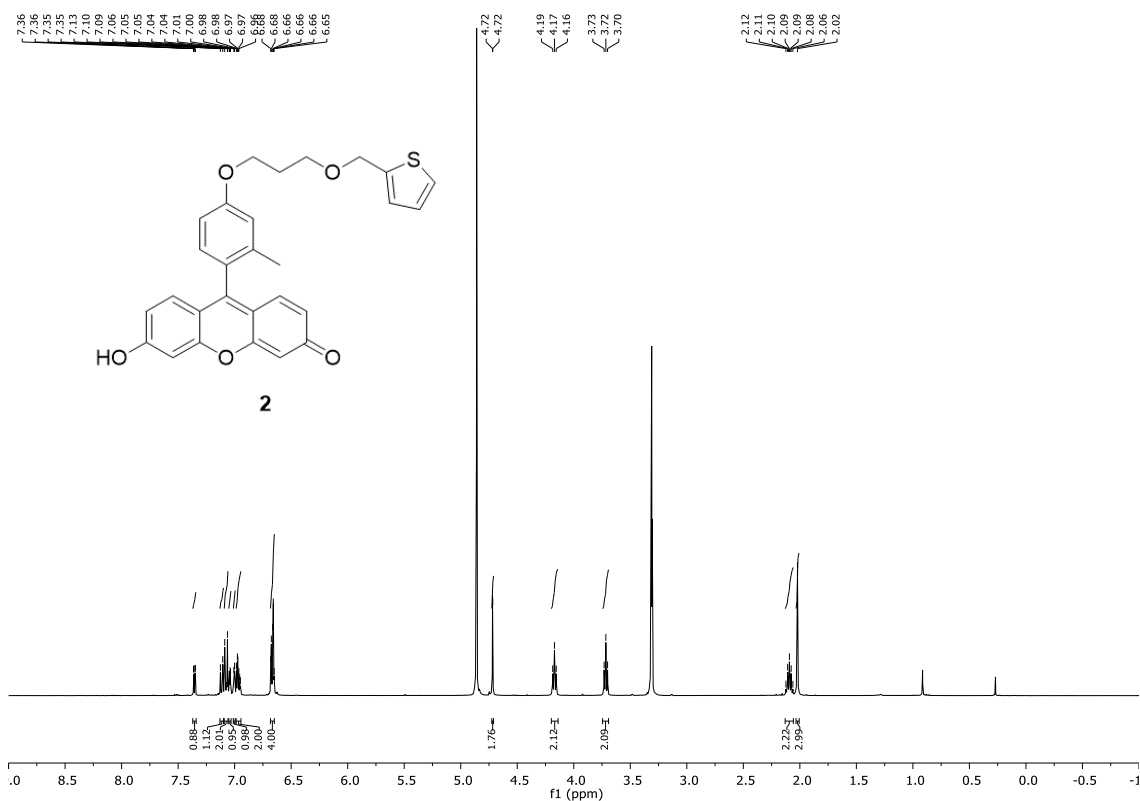
$^1\text{H-NMR}$ and $^{13}\text{C-NMR}$ spectra of compound **VII**. $^1\text{H NMR}$ (400 MHz, CDCl_3)



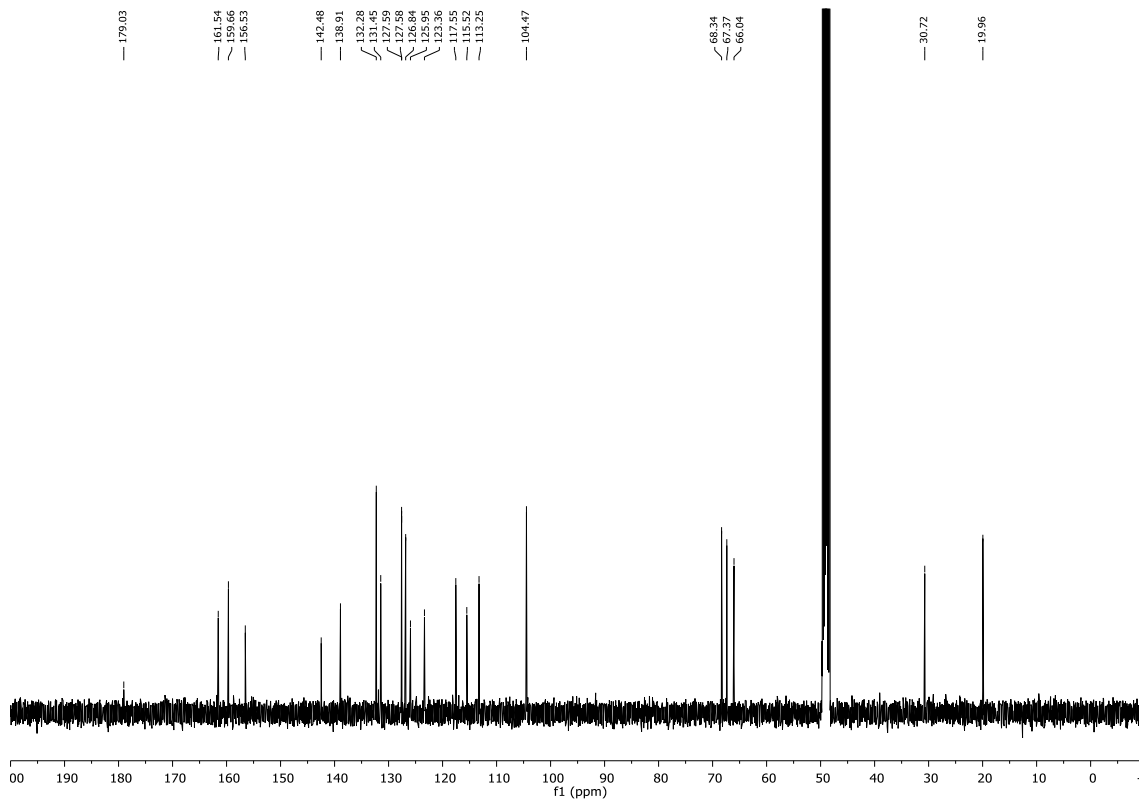
$^1\text{H-NMR}$ and $^{13}\text{C-NMR}$ spectra of compound **VII**. $^{13}\text{C NMR}$ (101 MHz, CDCl_3)



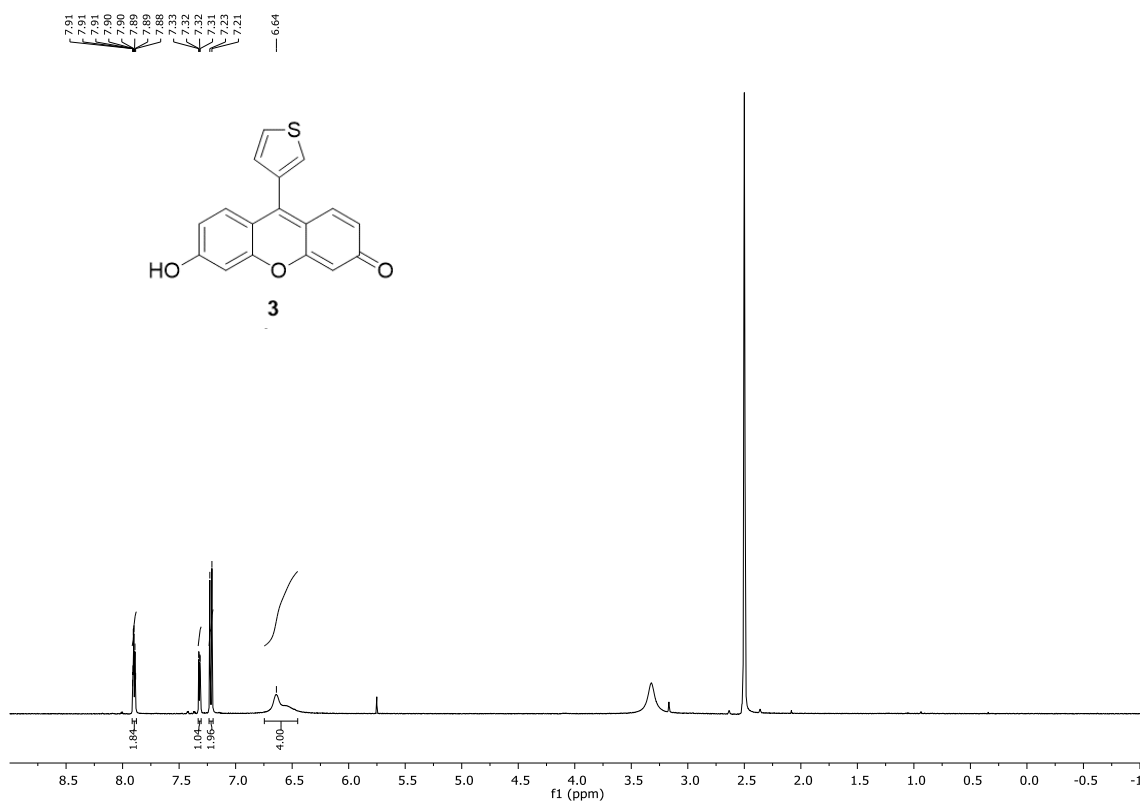
¹H-NMR and ¹³C-NMR spectra of compound 2. ¹H NMR (400 MHz, MeOD)



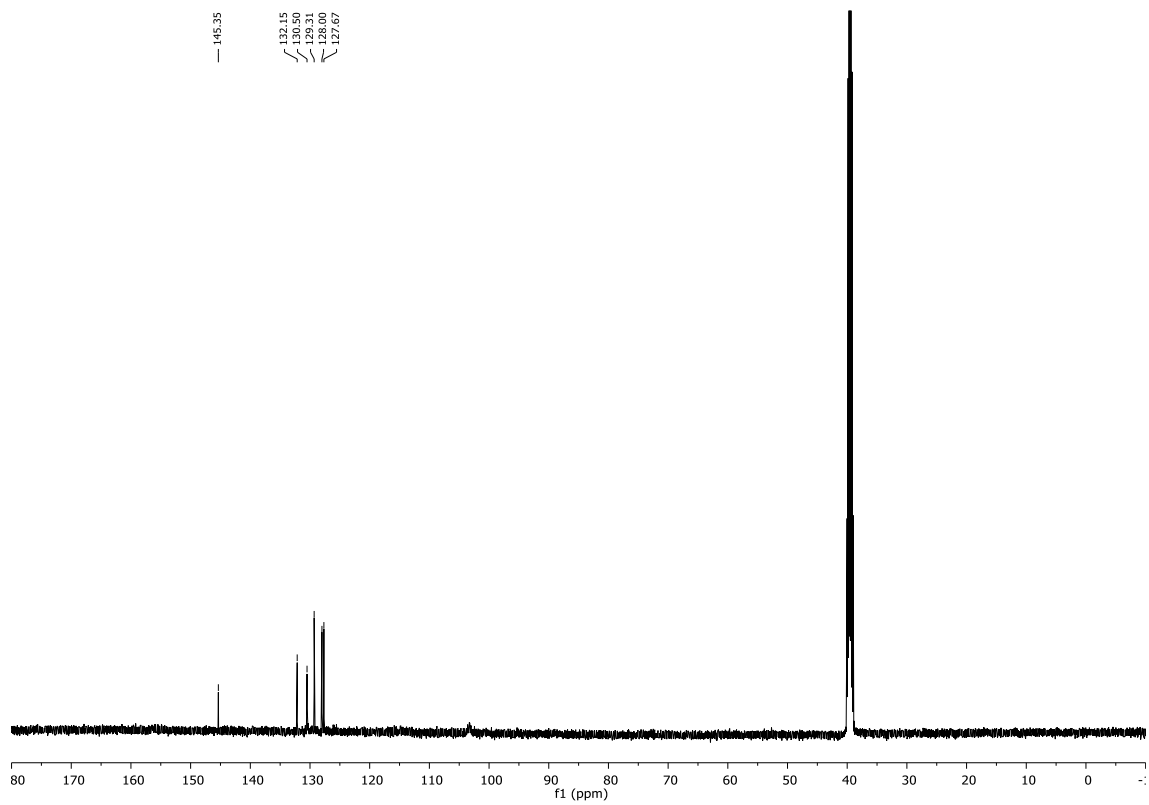
¹H-NMR and ¹³C-NMR spectra of compound 2. ¹³C NMR (101 MHz, CDCl₃)



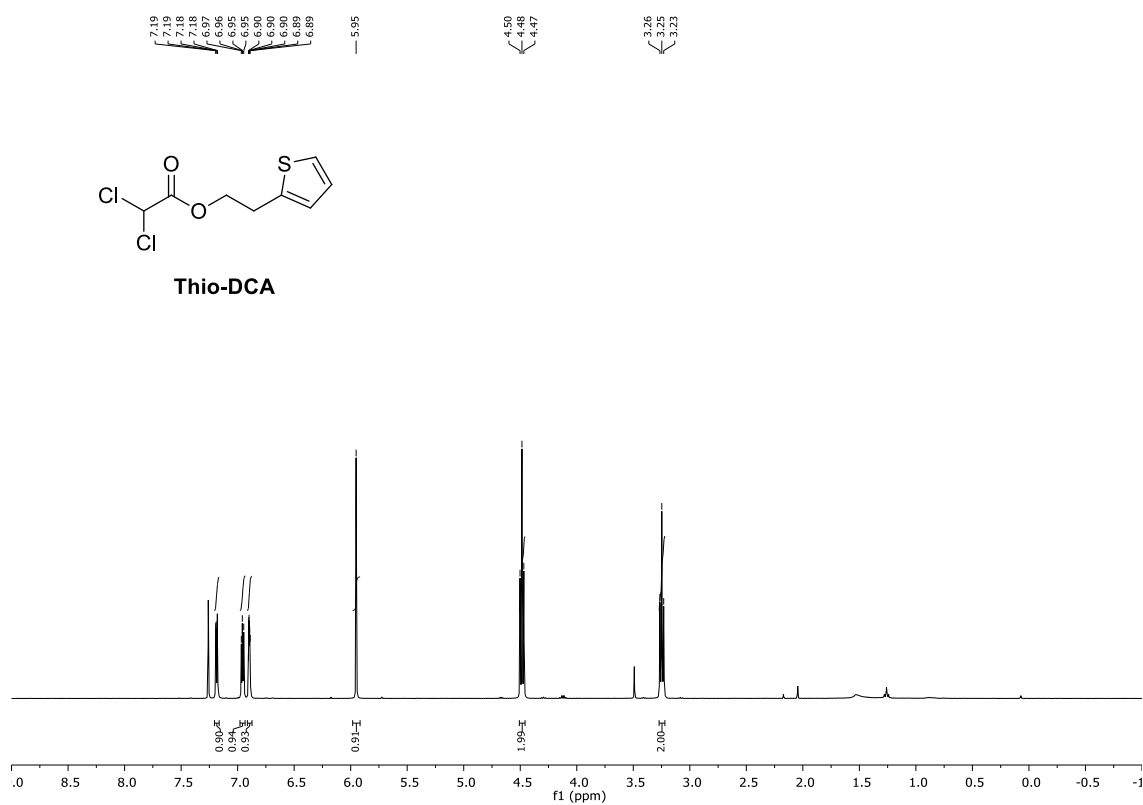
$^1\text{H-NMR}$ and $^{13}\text{C-NMR}$ spectra of compound **3**. $^1\text{H NMR}$ (500 MHz, $\text{DMSO-}d_6$)



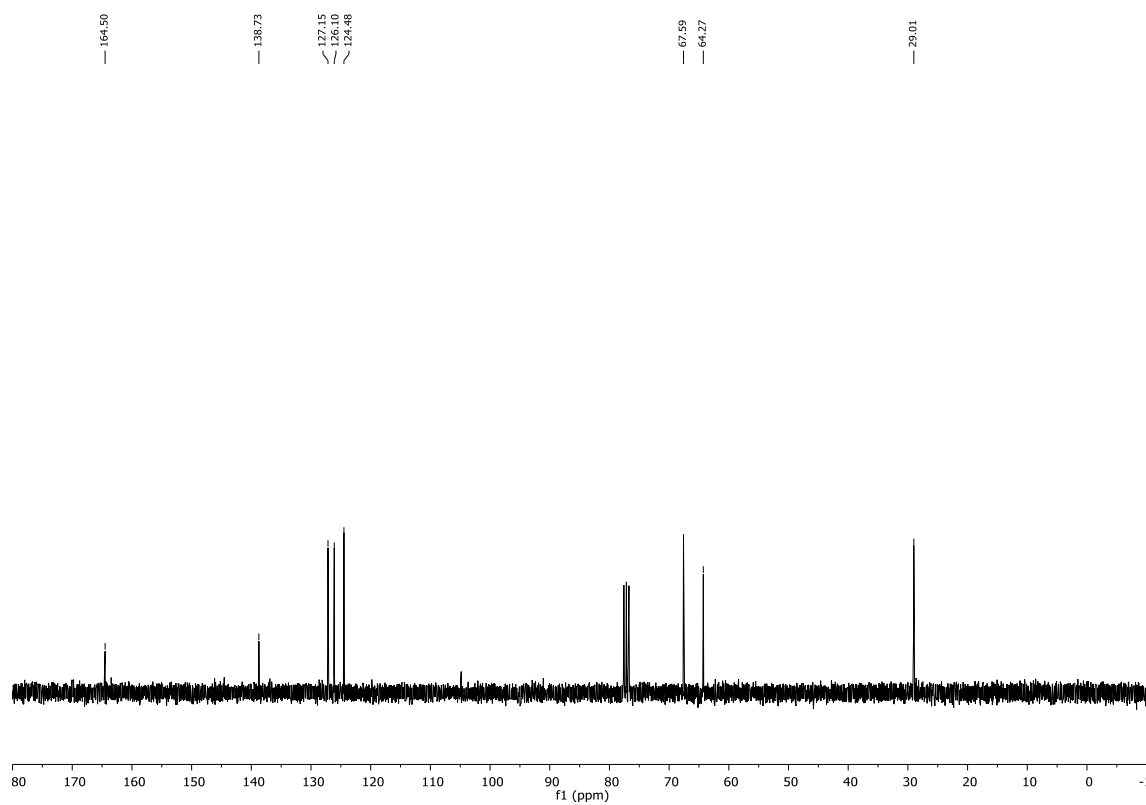
$^1\text{H-NMR}$ and $^{13}\text{C-NMR}$ spectra of compound **3**. $^{13}\text{C NMR}$ (126 MHz, $\text{DMSO-}d_6$)



$^1\text{H-NMR}$ and $^{13}\text{C-NMR}$ spectra of compound **Thio-DCA**. $^1\text{H NMR}$ (400 MHz, CDCl_3)



$^1\text{H-NMR}$ and $^{13}\text{C-NMR}$ spectra of compound **Thio-DCA**. $^{13}\text{C NMR}$ (75 MHz, CDCl_3)



S3. SUPPLEMENTARY EXPERIMENTAL PROCEDURES

S3.1. SPECTROSCOPY MEASUREMENTS

Absorption spectra of the different dyes in aqueous solutions were obtained on a Lambda 650 UV–visible spectrophotometer (PerkinElmer, Waltham, USA). The steady-state fluorescence emission and excitation spectra were collected using a Jasco FP-8300 spectrofluorometer (Jasco, Japan). Time-resolved fluorescence decay traces were obtained on a FluoTime 200 (PicoQuant GmbH, Germany), equipped with 375-nm, 440-nm, 470-nm, and 485-nm pulsed diode lasers as excitation sources, controlled by a PDL-800 laser driver (PicoQuant). Fluorescence decay traces were collected at three different emission wavelengths around the emission maximum of each dye, up to a total of 2×10^4 counts at the peak channel and using a 34 ps/channel time resolution. Global analysis was performed for an accurate determination of the fluorescence lifetimes.

Aqueous phosphate buffer (Sigma-Aldrich) and Tris buffer (Sigma-Aldrich) were prepared by dilution of the commercial concentrate solution to the final 10 mM concentration, and the pH dropwise adjusted using 1 M solutions of HCl or NaOH. For the measurements of dye **3** in methanol:glycerine mixtures of different viscosity, the mixtures were prepared using different proportions ranging from 100% (v/v) methanol to 99% (v/v) glycerine. The density and viscosity of the mixtures were measured in quintuplicate using floating pycnometers and a Hoppler viscosimeter, respectively, at three different temperatures, on a temperature-controlled water bath.

S3.2. DUAL-COLOR CONFOCAL FLUORESCENCE MICROSCOPY

Multicolor confocal imaging of cells stained with MT and compound **2** or **3** was performed using a laser scanning microscope (Fluoview FV1000, Olympus, Tokyo, Japan). A 60x water immersion objective (UPLSAPO, NA = 1.20) was used for all the experiments. For imaging compound **2**, compound **3** or MT, the sample was excited with a 405 nm, 488 nm or 635 nm laser line, respectively. The excitation light was reflected using a DM405/488/559/635 dichroic (Olympus). The fluorescence from the synthesized compounds and MT was split using an SDM 510 or SDM 560 dichroic for compound **2** or **3**, respectively. Emission from compound **2** was collected between 410 and 490 nm, and emission from compound **3** was collected between 500 and 580 nm using a grating. For MT, a BA655-755 bandpass filter was used. To minimize the crosstalk between the channels, image acquisition was performed using consecutive excitation.

S3.3. DUAL-COLOR FLUORESCENCE LIFETIME IMAGING MICROSCOPY (FLIM)

Colocalization studies using dual-color FLIM were performed on a MicroTime 200 fluorescence lifetime microscope system (PicoQuant). Different pulsed diode lasers were employed as excitation sources (all from the LDH series from PicoQuant), depending on the dye to be imaged (see Table S1). The laser heads were controlled with a Sepia II driver (PicoQuant) working at a 10 or 20 MHz repetition rate. When dual-color pulsed interleaved excitation (PIE) [7] was possible, for the alternating excitation of the studied dye and the MitoTracker Deep Red (MT) dye (Life Technologies, Carlsbad, CA, USA), the 635-nm pulsed laser (LDH-P-635, PicoQuant) was delayed to the middle of the detection window using a delay box (ORTEC DB463 delay box, Ametek, USA). The excitation laser beams were directed into the specimen through an apochromatic oil immersion objective (100 \times , 1.4NA) of an inverted microscope system (IX-71, Olympus, Japan). The fluorescence light was collected back and filtered through the main dichroic and cut-off filters and spatially filtered through a 75- μ m pinhole. Finally, the fluorescence was separated into two detection channels using a dichroic mirror or beam splitter; the first channel was dedicated to the tested fluorescent probe, whereas the second channel was dedicated to the red fluorescence from MT. Two single-photon avalanche diodes (SPCM-AQR 14, Perkin-Elmer Optoelectronics, USA) were used as photon detection devices. Imaging

reconstruction, photon counting, and data acquisition were realized using a TimeHarp 200 card (PicoQuant). The different areas were raster-scanned using a 512×512 pixel resolution, and a 60 ms/pixel acquisition time. FLIM analyses were performed by fitting the fluorescence decay traces obtained in the individual pixels, after a 5×5 spatial binning, to a single exponential decay function using a reconstructed instrument response function and a parameter optimization based on the maximum likelihood estimator (MLE). FLIM imaging and colocalization image analyses were performed using home-coded scripts in SymPhoTime 32 (PicoQuant), MathCad 15.0 (PTC, USA) and FiJi (distribution of ImageJ) [8, 9].

Table S1. Dual-color FLIM instrumental settings for colocalization studies of each dye

Compound ^[a]	Excitation sources ^[b]	Main dichroic	Cut-off filter	Detection channel splitter	Filter in dye's channel	Filter in MT's channel
1	440 nm	440DCR	LP460	600DCXR	465/30	685/70
2–4	470 nm/635 nm in PIE	470/635 dual-band	LP500	600DCXR	520/35	685/70

^[a] See Chart 1 for structures. ^[b] PIE: Pulsed interleaved excitation.

S3.4. CELL CULTURE FOR FLUORESCENCE IMAGING

The human osteosarcoma cell line 143B was obtained from the American Type Culture Collection (ATCC; CRL-8303). The cells were cultured with high glucose Dulbecco's modified Eagle's medium (DMEM) containing GlutaMAX-I (4 mM), sodium pyruvate (1 mM) (GIBCO, Life Sciences), 1% penicillin/streptomycin (GIBCO, Life Sciences), and 10% fetal bovine serum (FBS) (GIBCO, Life Sciences). The cells were subcultured every 3-4 days at a density of 2.4 or 5.6×10³ cells/cm², and the media were refreshed the day before subculture.

ρ₀206 cells were obtained from the parental osteosarcoma line 143B. These cells are depleted of mitochondrial DNA as a result of long-term passaging in the presence of low concentrations of ethidium bromide [10]. Accordingly, the genes for oxidative phosphorylation and mitochondrial respiration are knocked out of ρ₀206 cells. The cells have mitochondrial organelles, but their metabolism is totally adapted for survival and to maintain their proliferative capacity. ρ₀206 cells were kindly obtained from Giuseppe Attardi's laboratory. The cells were cultured in high-glucose DMEM containing GlutaMAX-I (4 mM), sodium pyruvate (1 mM) (GIBCO, Life Sciences), 2% penicillin/streptomycin (GIBCO, Life Sciences), and 10% FBS (GIBCO, Life Sciences). The cells also require an exogenous addition of 0.5% uridine (Sigma-Aldrich) and an extra concentration of sodium pyruvate (1 mM). The cells were subcultured every 3-4 days at a density of 5.6×10³ or 1×10⁴ cells/cm², and the media were refreshed the day before subculture.

MDA-MB-231 and SKBR-3 were obtained from the ATCC (HTB-26 and HTB-30). The cell line SKBR3 was cultured with modified McCoy's 5A medium, 1% glutamine (GIBCO, Life Sciences), 1% penicillin/streptomycin (GIBCO, Life Sciences), and 10% FBS (GIBCO, Life Sciences). The cell line MDA-MB-231 was cultured in high-glucose DMEM containing GlutaMAX-I (4 mM), sodium pyruvate (1 mM) (GIBCO, Life Sciences), 1% penicillin/streptomycin (GIBCO, Life Sciences), and 10% FBS (GIBCO, Life Sciences). The cells were subcultured every 3-4 days at a density of 1.35 or 1.1×10⁶ cells/cm², and the media were refreshed the day before subculture.

HeLa cells were maintained in DMEM without phenol red (Life Technologies) and supplemented with 10% FBS (Life Technologies) at 37 °C under a humidified 5% CO₂ atmosphere. Before image acquisition the cells were washed 3 times with 1 mL of Hank's balanced salt solution (HBSS) (Life Technologies). The dye was added for 5 min and washed with HBSS. After that, 4% formaldehyde was added for cell fixation. After 30 min, the cells were washed with HBSS. Staining with the mitochondria tracker MT was performed according to the manufacturer's instructions. For imaging, cells were seeded in 35-mm, glass-bottom dishes (MatTeK, USA). Imaging was performed in HBSS at room temperature unless otherwise specified.

S3.5. IMAGE ANALYSIS

Image analysis and segmentation was performed as described previously [11, 12], using home-scripted macros in *Fiji is just imagej* [8]. In brief, background subtraction was performed by previously applying a 20×20 pixel median filter [13] and a subsequent manual threshold selection to select the regions of interest of both images (dye and MT).

The Pearson coefficient (r) was obtained through the next equation:

$$r = \frac{\sum(x-\bar{x})(y-\bar{y})}{\sqrt{\sum(x-\bar{x})^2 \sum(y-\bar{y})^2}} \quad (\text{S1})$$

Where x and y are the pixel intensity values of the first and second images respectively and \bar{x} and \bar{y} are the mean of all the pixel matrix. We calculated r using a home-made macro in *Fiji is just imagej* by obtaining the matrices $(x - \bar{x})$, $(y - \bar{y})$, $(x - \bar{x})^2$ and $(y - \bar{y})^2$ after applying the threshold.

Mander's colocalization coefficients were obtained to indicate the amount of mutually colocalized pixels for each channel using the JACoP plugin [14] in *Fiji is just imagej*.

These treated images were stacked for visual inspection of colocalization, and obtain the segmented masks of coincident (assigned to mitochondria) or noncoincident pixels. These masks were subsequently applied to the dye's lifetime matrix to extract the lifetime distributions in each region.

S3.6. CELL VIABILITY ASSAYS

The DCA or **Thio-DCA** compounds were diluted in DMSO to a concentration of 2 M, and a working 0.25 M solution was subsequently prepared in phosphate buffered saline (PBS). The effect of the DCA or **Thio-DCA** compounds on cell viability was studied using the CellTiter Blue™ viability assay (Promega). The cells were plated in quadruplicate in black, cell culture-treated, 96-well, optical, flat-bottom plates at a density of 8×10⁴ cells/well. The studied compounds were added directly to the wells at different concentrations (1.25, 2.5, 5, 7.5, and 10 mM). After incubation in the presence of the drug for 96 h at 37 °C, 20% v/v CellTiter-Blue™ (Promega) reagent was added to the wells, followed by further incubation for 2 h at 37 °C. Finally, the fluorescence emission was directly read at 520 nm excitation and 610/30 nm emission in a Glomax® Multidetector System (Promega). Untreated cell controls (containing the same amount of DMSO as the treated wells) and wells with only reagents served as background controls and were run together with the treated cells. The absolute fluorescence was recorded in arbitrary units and the data were subsequently expressed as percentages relative to the untreated control cells. At least five independent repetitions of each data point were obtained. The significance of the differences in viability with the different treatments with respect to the controls was obtained using the Holm-Bonferroni and Holm-Sidak tests and the non-parametric Kolmogorov-Smirnov and Mann-Whitney tests in Origin 9.0 (OriginLab Co., USA).

S.4. SUPPLEMENTARY SPECTROSCOPY FIGURES OF DYES 1-4

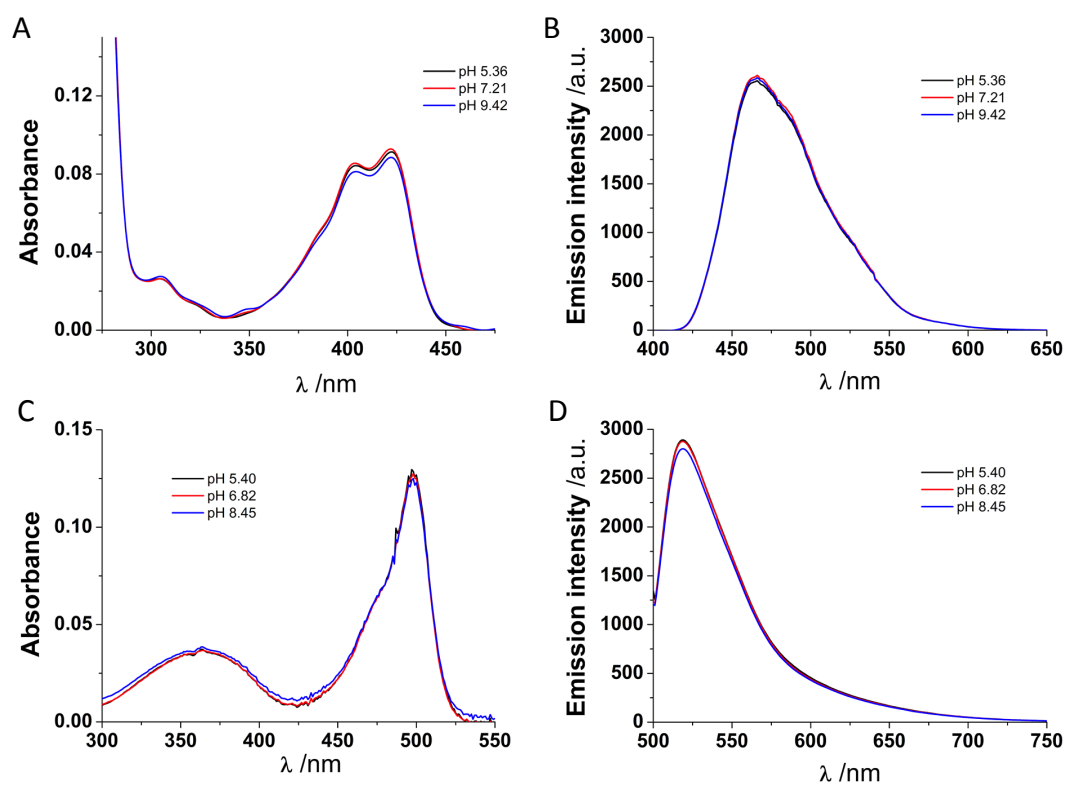


Figure S1. Absorption (A, C) and fluorescence emission (B, D) spectra of dyes 1 (A, B) and 4 (C, D) at different pH values.

The excitation wavelength for the emission spectra was 375 nm for compound 1 and 495 nm for compound 4.

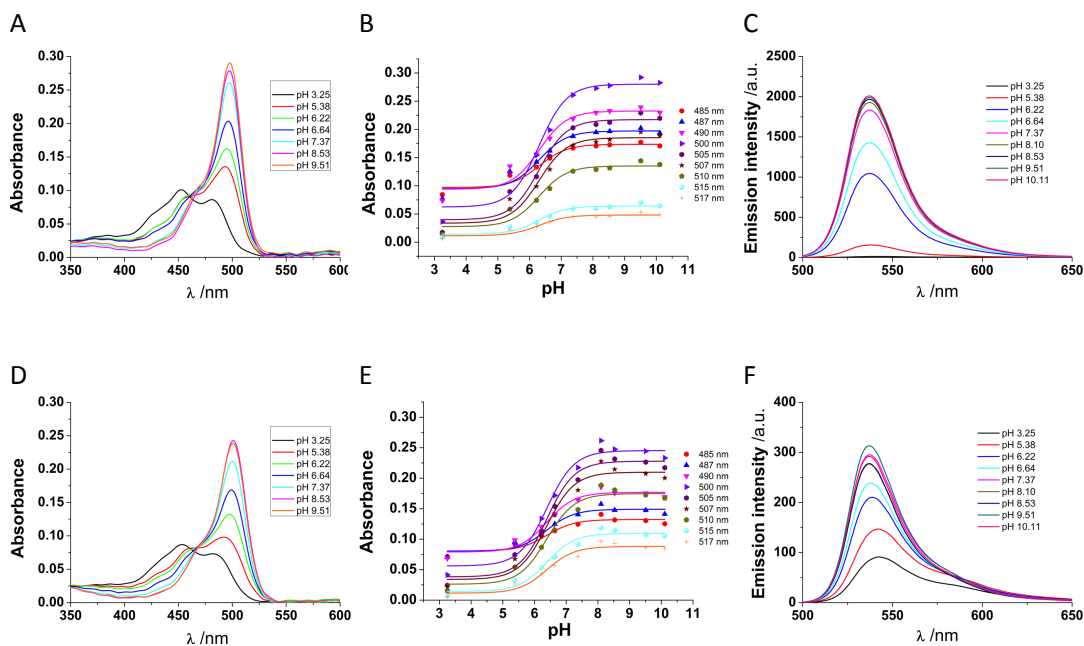


Figure S2. Absorption and fluorescence emission dependence with pH of dyes **2** (A-C) and **3** (D-F) in aqueous solution.

A and D) Absorption spectra at different pH values of dyes **2** (A) and **3** (D). B and E) Global fittings of the A vs pH data to the general equilibrium equations [15, 16] to obtain the ground state pK_a values of dyes **2** (B) and **3** (E). C and F) Fluorescence emission spectra ($\lambda_{ex} = 490$ nm) of dyes **2** (C) and **3** (F) in aqueous solution at different pH values.

S.5. VISCOSITY DEPENDENCE OF THE FLUORESCENCE LIFETIME OF DYE 3

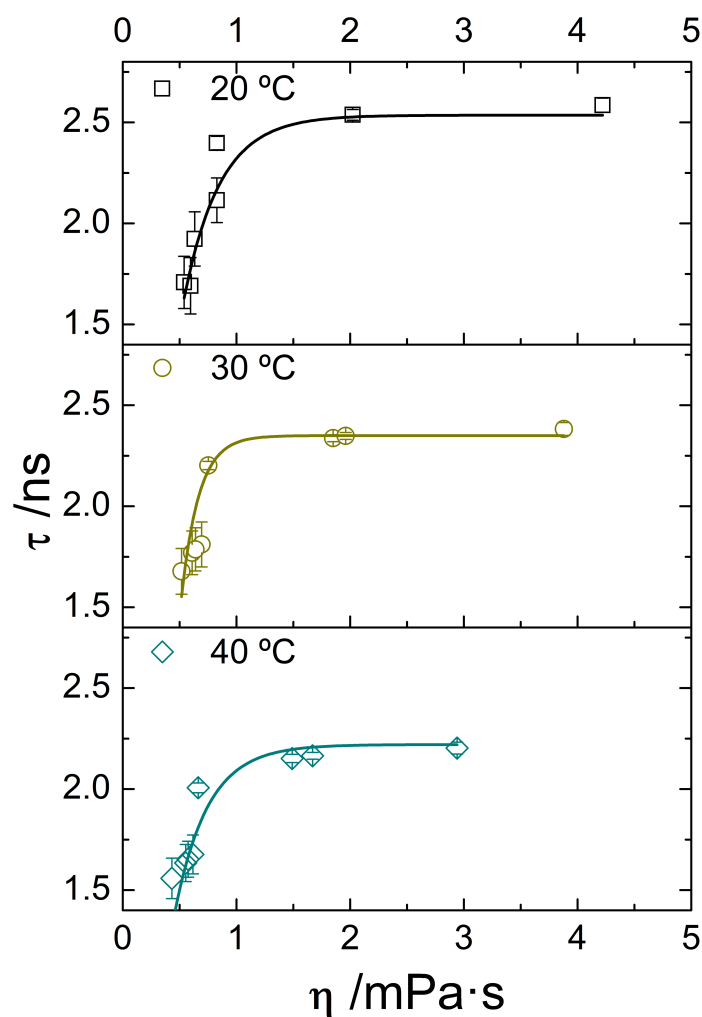


Figure S3. Average fluorescence lifetime, τ , of dye **3** in methanol:glycerine mixtures of different viscosity at 20, 30 and 40 °C.

Methanol:glycerine mixtures of different viscosity were prepared using different proportions ranging from 100% (v/v) methanol to 99% (v/v) glycerine. The density and viscosity values of the mixtures were experimentally measured as described in the supplementary methods. The faster deactivation of dye **3** in low-viscosity mixtures and the overall viscosity dependence of its τ values are related to the free rotation of the thiophene moiety with respect to the fluorophore xanthene core. Although this could serve as basis for the development of a viscosity sensor [17], the viscosity values to which dye **3** responds are lower than 1 mPa·s, which limits its use in biologically-relevant applications.

S.7. PHOTOSTABILITY OF DYES 1-4

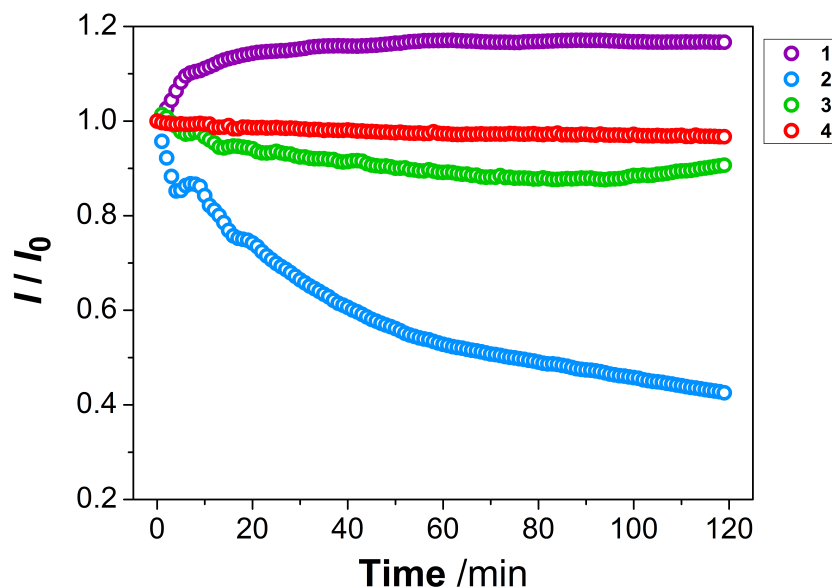


Figure S4. Photostability of dyes 1–4 during 2 h of continuous irradiation.

Fluorescence emission intensity was measured with $\lambda_{\text{ex}} = 407$ (for **1**) and 497 nm (for **2–4**). The excitation slit was open to 20 nm and the shutter was continuously open. The absorbance of the solutions was measured before the experiment, being in all cases lower than 0.1 at the λ_{ex} . Fluorescence emission spectra were collected every 5 min during 2 hours. Acridone **1** increased its emission by 16%, probably due to slow solubility. Xanthene derivative **2** was less photostable, showing a 57% decrease in intensity within the 2 h. In contrast, xanthene **3** and BODIPY **4** showed excellent photostability, exhibiting loss of fluorescence emission of 9 % (**3**) and 3 % (**4**), respectively. These results ensure that the dyes are not drastically photodamaged during the time span of fluorescence imaging experiments (less than 1 h).

S.7. ADDITIONAL COLOCALIZATION STUDIES OF DYES 1-4 WITH MT

The following Supplementary Figures show additional results of the colocalization of the studied dyes, 1–4, with the mitochondria tracker dye MT using either dual-color confocal or dual-color FLIM.

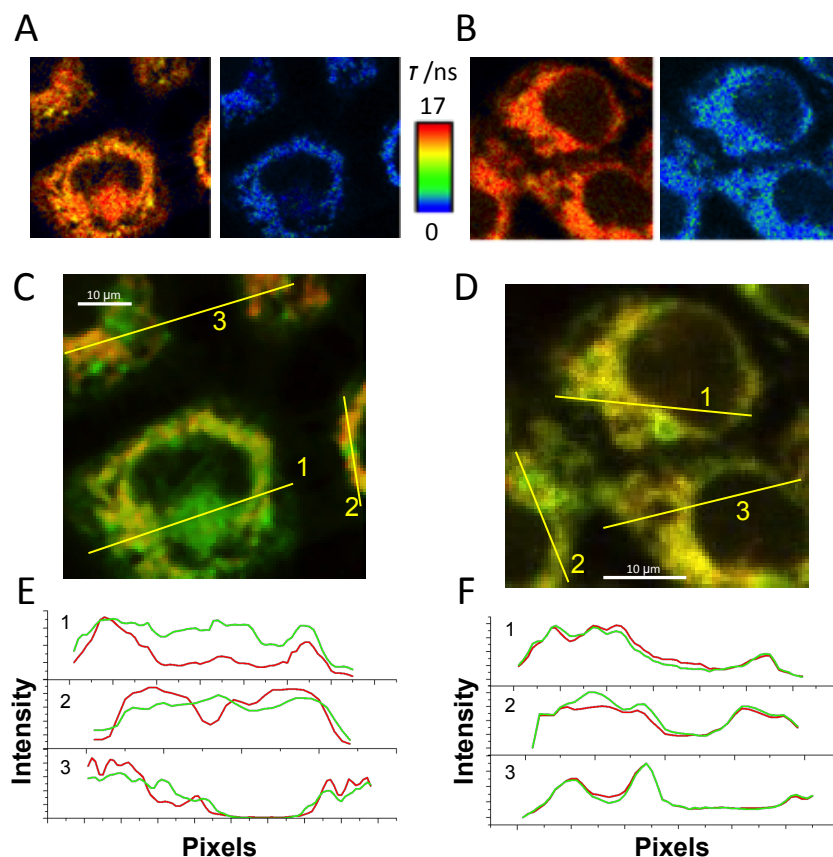


Figure S5. Representative dual-color FLIM images of compound 1 in 143B cells and ρ_0206 cells after 20 min of incubation with MT.

Panels (A) and (B) show FLIM images on a pseudo-color scale (between 0 and 17 ns) of the dye's detection channel (left) and the MT detection channel (right). These examples were performed on human osteosarcoma 143B cells (A) and ρ_0206 cells (B). The latter are tumor cells depleted of mitochondrial DNA, thus displaying an extreme metabolic phenotype due to the absence of respiration [10].

Panels (C) and (D) show the colocalization images of 1 (green) and MT (red) in 143B cells (C) and ρ_0206 cells (D). Intensity traces in both channels are shown for the depicted lines in panels E (for 143B cells) and F (for ρ_0206 cells). Scale bars represent 10 μm .

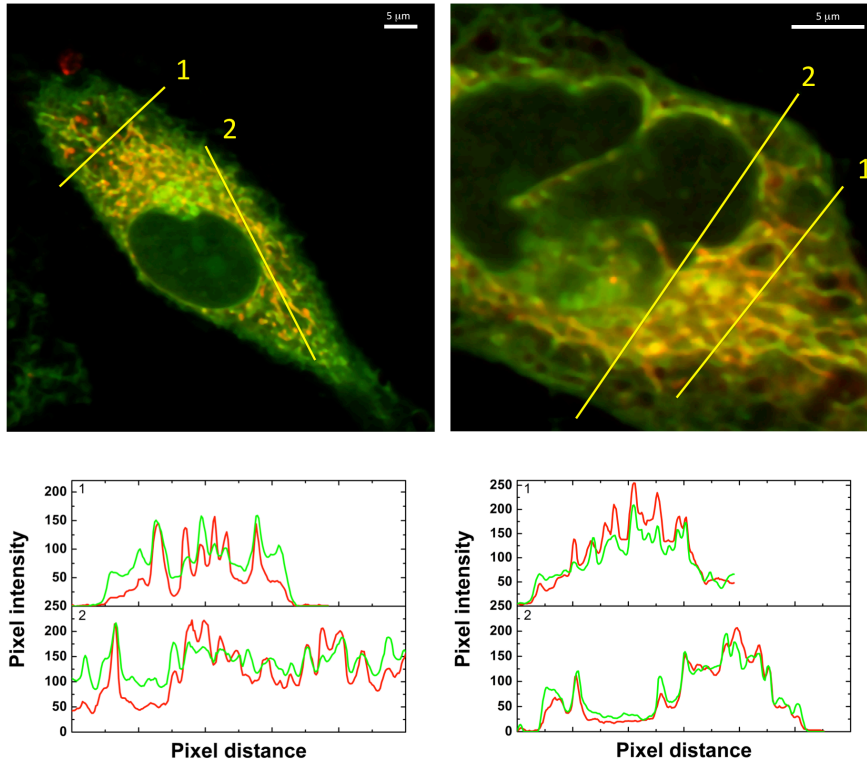


Figure S6. Representative dual-color, super-resolution optical fluctuation imaging (SOFI) of **1** (green channel) and MT (red channel) in formaldehyde-fixed HeLa cells, and intensity plots of the profile lines.

Scale bars represent 5 μm.

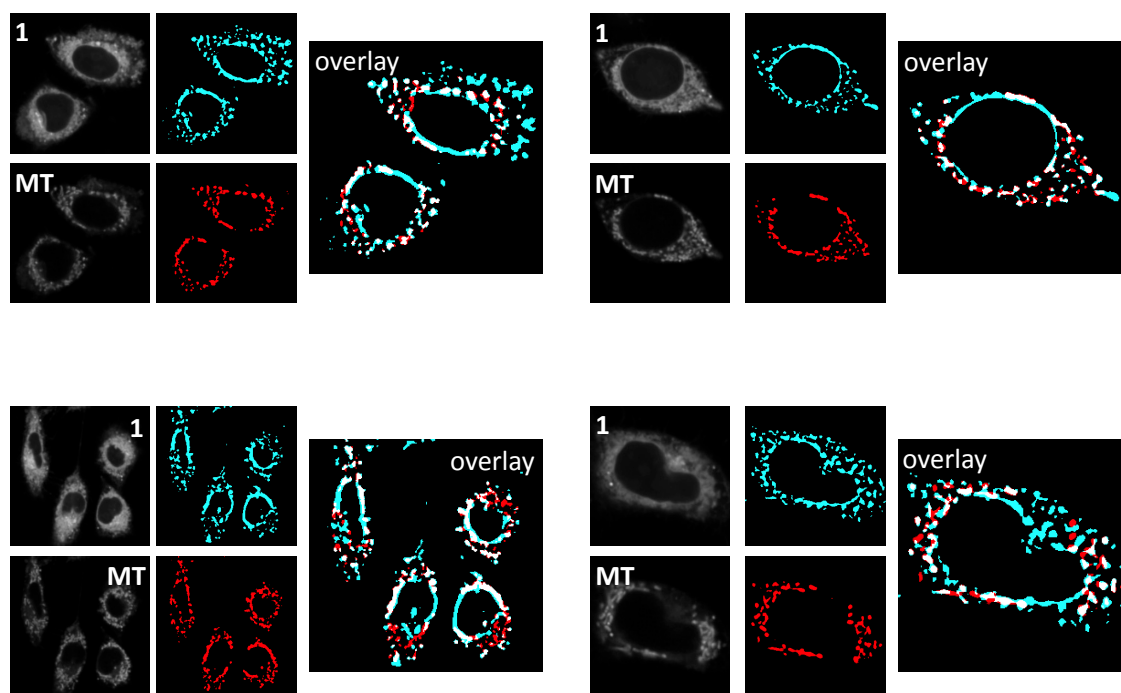


Figure S7. Mitochondrial localization of compound **1** in 143B cells, after 20 min of incubation with MT, from dual-color FLIM images.

Left panels represent the raw intensity images in the **1** channel and the MT channel. Central panels represent the selected region of interest, in cyan for compound **1** and red for MT. Rightmost panels are the overlaid images, with colocalized pixels represented in white color.

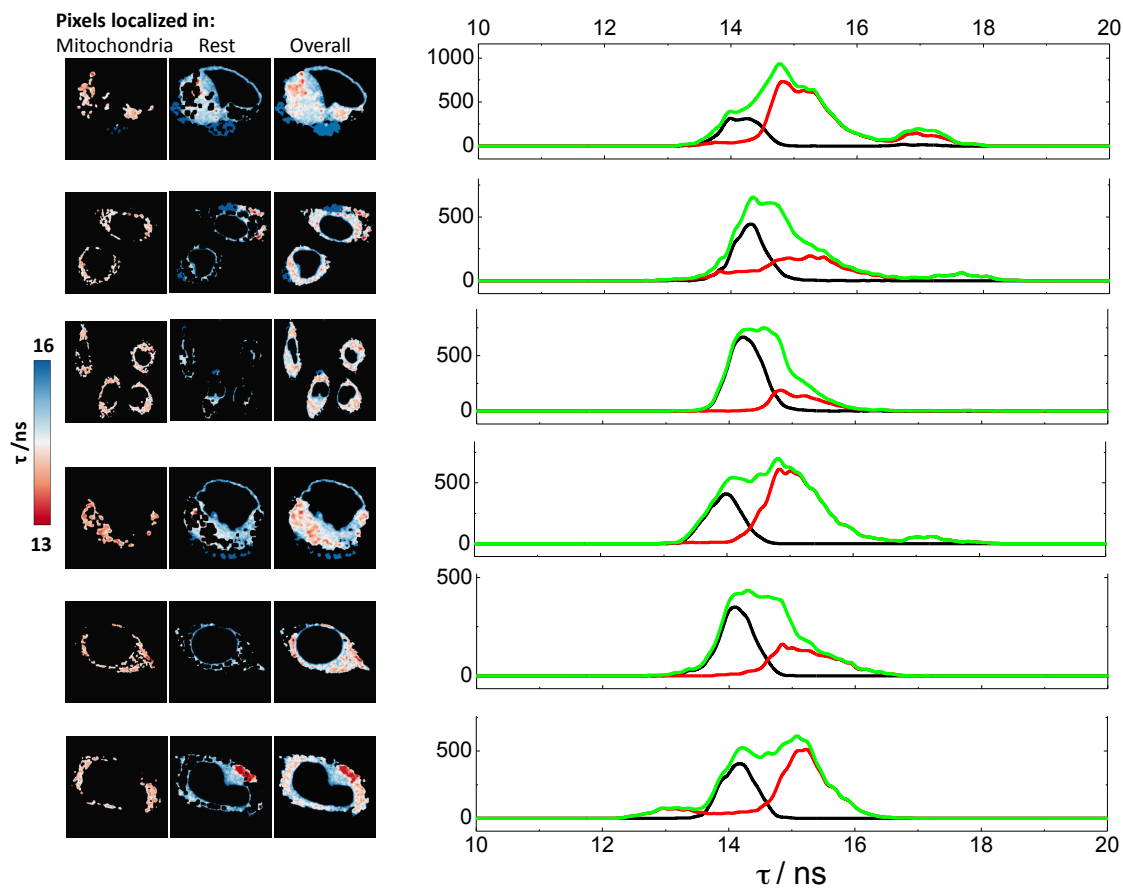


Figure S8. FLIM imaging of compound **1** in 143B cells.

The images show the fluorescence lifetime of **1** depicted on a pseudocolor scale between 13 and 16 ns. The leftmost column of images shows the colocalized pixels with mitochondria. The central column of images shows the non colocalized pixels. The rightmost column of images shows the overall images. The plots on the right panels represent the pixel distribution of fluorescence lifetime of **1** in each image, localized in mitochondria (black lines) or in other cellular subcompartments (red lines), and the overall lifetime distribution (green lines). Given that the acridone core has a lifetime that depends on the polarity of the microenvironment [18], these data clearly show that the mitochondria matrix is a less polar environment than cellular cytoplasm.

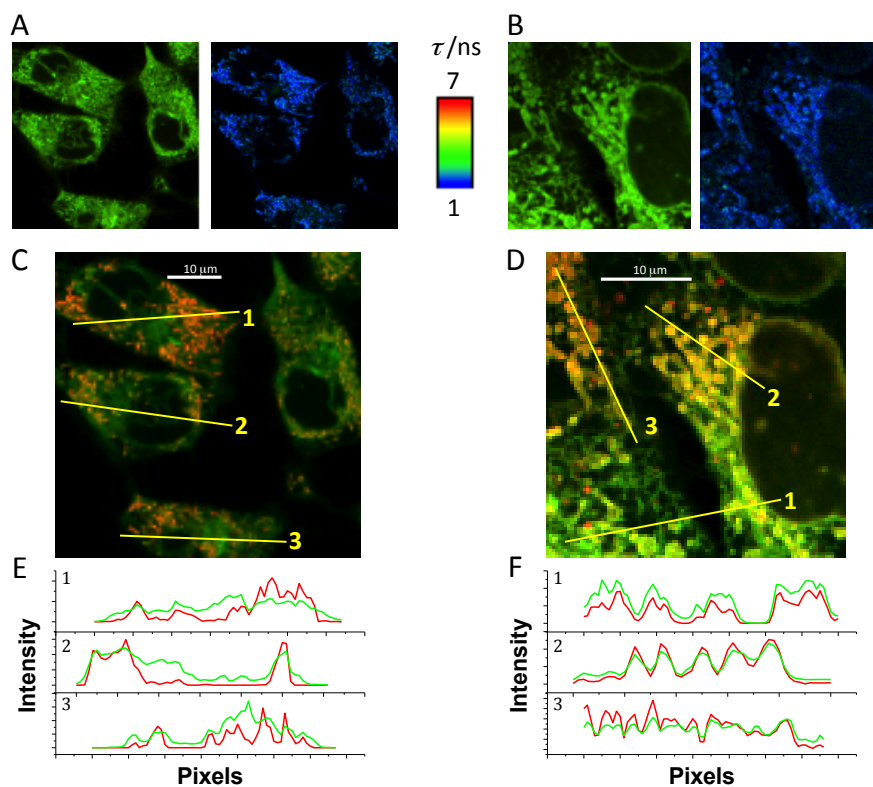


Figure S9. Representative dual-color FLIM images of compound **2** in 143B (A, C, and E) and ρ_0206 cells (B, D, and F), after 20 min of incubation with MT.

In the FLIM images (A and B), the dye's detection channel (left) and the MT detection channel (right) are shown separately. The colocalization images (C and D) of the dye (green) and MT (red) are also shown. Intensity traces in both channels (E and F) are shown for the depicted lines in the colocalization panels. Scale bars represent 10 μm .

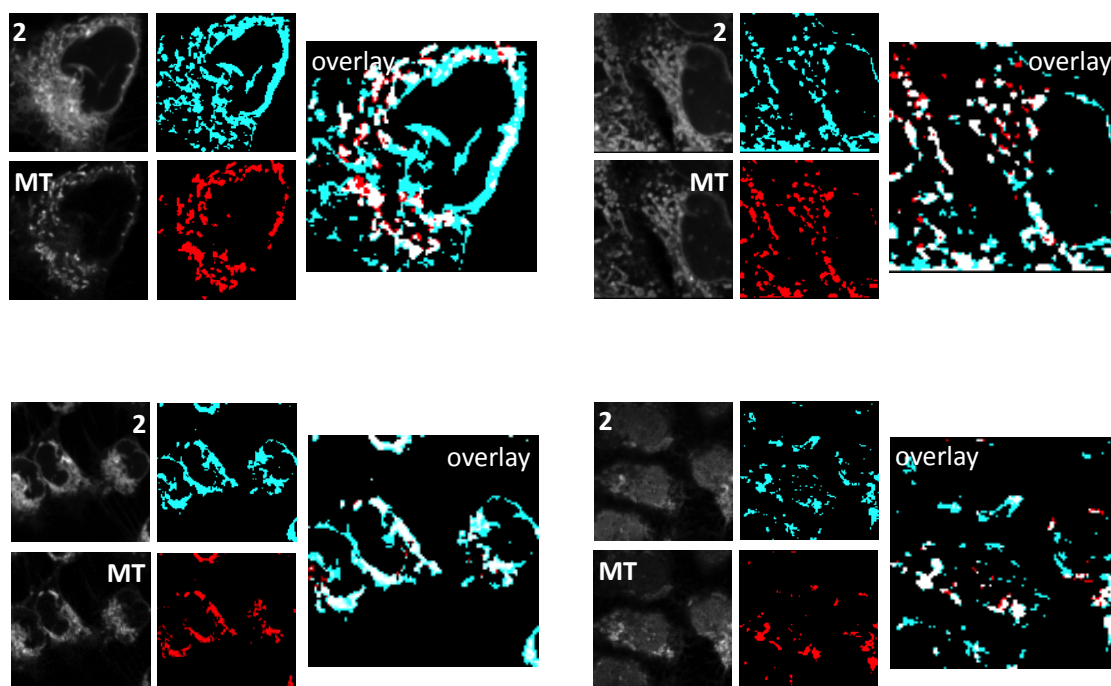


Figure S10. Mitochondrial localization of compound **2** in ρ_0206 cells, after 20 min of incubation with MT, from dual-color FLIM images.

Left panels represent the raw intensity images in the **2** channel and the MT channel. Central panels represent the selected region of interest, in cyan for compound **2** and red for MT. Rightmost panels are the overlaid images, with colocalized pixels represented in white color.

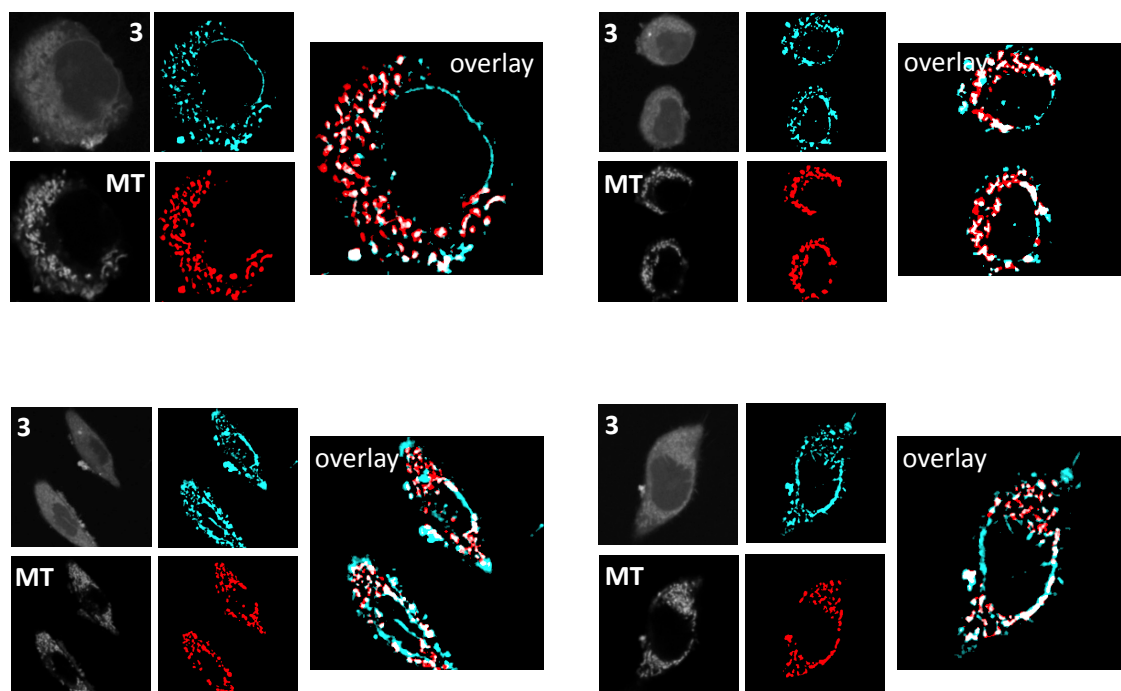


Figure S11. Mitochondrial localization of compound **3** in MDA-MB-231 cells, after 20 min of incubation with MT, from dual-color FLIM images.

Left panels represent the raw intensity images in the **3** channel and the MT channel. Central panels represent the selected region of interest, in cyan for compound **3** and red for MT. Rightmost panels are the overlaid images, with colocalized pixels represented in white color.

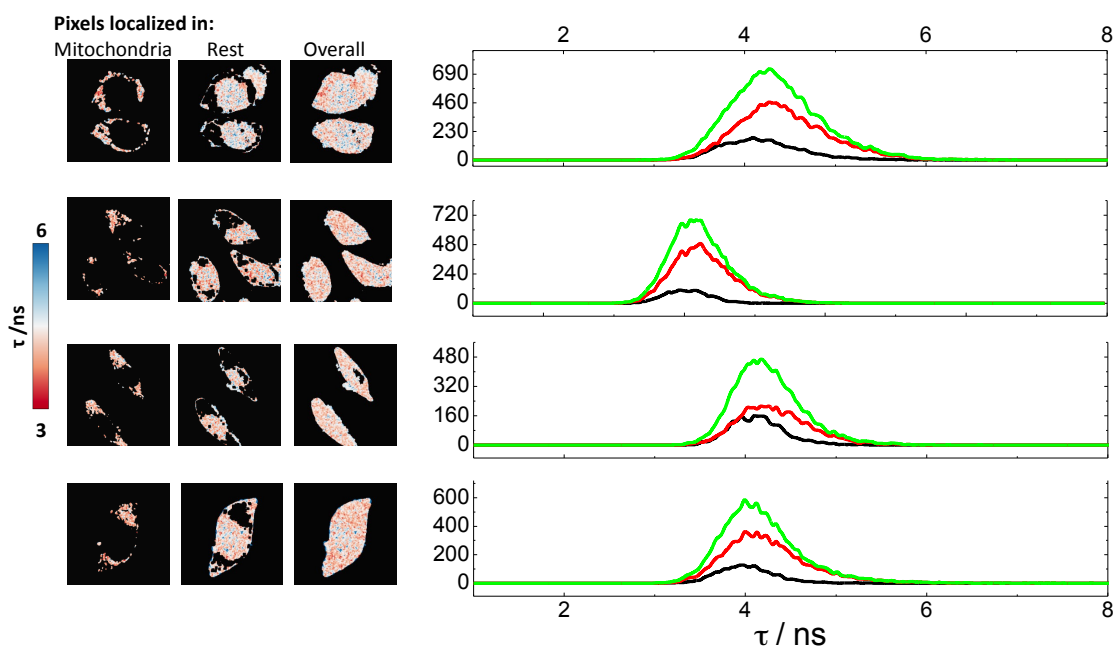


Figure S12. FLIM imaging of compound **3** in MDA-MB-231 cells.

The images show the fluorescence lifetime of **3** depicted on a pseudocolor scale between 3 and 6 ns. The leftmost column of images shows the colocalized pixels with mitochondria. The central column of images shows the non colocalized pixels. The rightmost column of images shows the overall images. The plots on the right panels represent the pixel distribution of fluorescence lifetime of **3** in each image, localized in mitochondria (black lines) or in other cellular subcompartments (red lines), and the overall lifetime distribution (green lines).

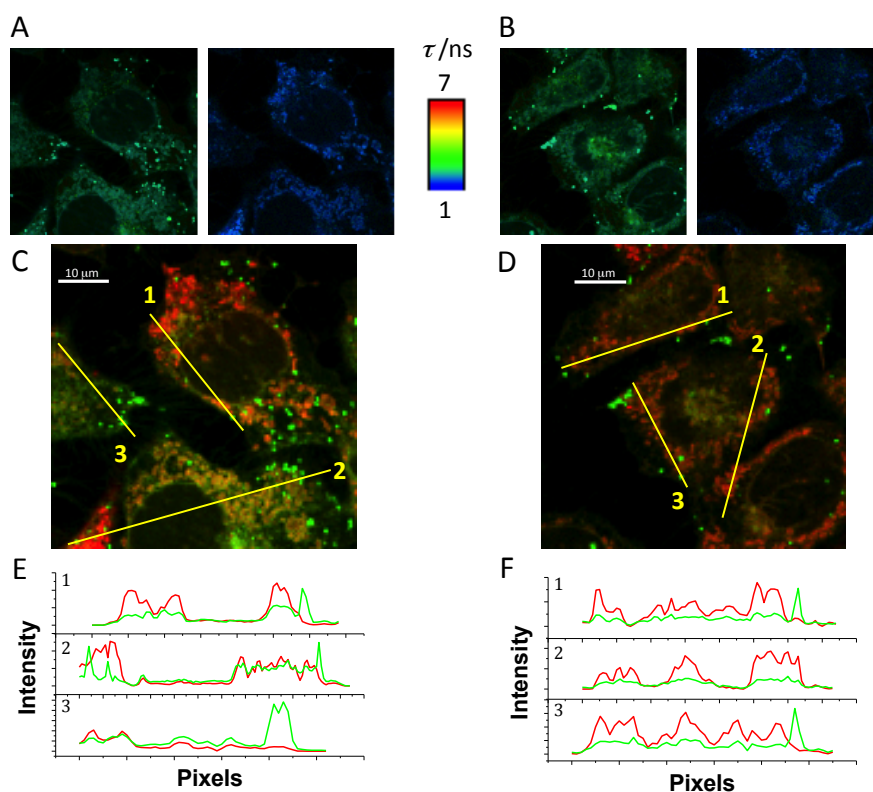


Figure S13. Representative dual-color FLIM images of compound **4** in 143B (A, C, and E) and ρ_0206 cells (B, D, and F), after 20 min of incubation with MT.

In the FLIM images (A and B), the dye's detection channel (left) and the MT detection channel (right) are shown separately. The colocalization images (C and D) of the dye (green) and MT (red) are also shown. Intensity traces in both channels (E and F) are shown for the depicted lines in the colocalization panels. Scale bars represent 10 μm .

Table S2. Pearson's correlation coefficient (PCC) and Manders' colocalization coefficient (MCC) values for the colocalization of dyes **1–4** with the mitochondria tracker MT.^[a]

Compound	PCC	MCC dye channel	MCC MT channel
1	0.59±0.10	0.46±0.14	0.64±0.10
2	0.69±0.07	0.64±0.14	0.73±0.14
3	0.58±0.12	0.58±0.15	0.66±0.12
4	0.67±0.04	0.46±0.06	0.36±0.12

^[a] All the values are averages from, at least, five different images. Errors are reported as standard deviation.

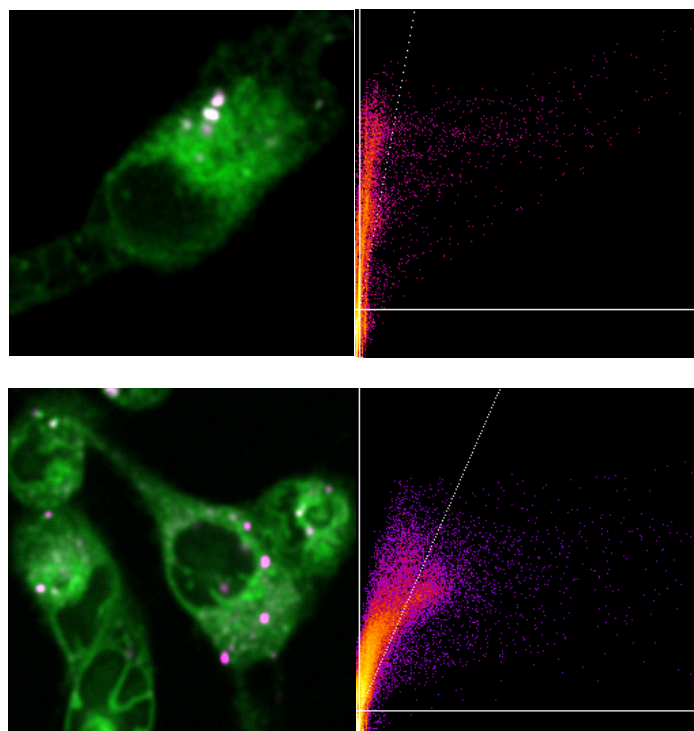


Figure S14. Representative dual-color fluorescence images of compound **1** (green) and the MT tracker (magenta) in 143B cells after 20 min of incubation with BAM15.

Scatter plots represent the correlation of the intensity values in the green channel vs the red channel. Scale bars represent 10 μm .

REFERENCES

- [1] C. Chen, S.H. Hong, Selective catalytic sp³ C-O bond cleavage with C-N bond formation in 3-alkoxy-1-propanols, *Org Lett*, 14 (2012) 2992-5. doi: 10.1021/ol3009842.
- [2] H.V. Huynh, Y.X. Chew, Synthesis, structural characterization and catalytic activity of a palladium(II) complex bearing a new ditopic thiophene-N-heterocyclic carbene ligand, *Inorg Chim Acta*, 363 (2010) 1979-83. doi: <https://doi.org/10.1016/j.ica.2009.02.035>.
- [3] J.A. Smith, R.M. West, M. Allen, Acridones and quinacridones: novel fluorophores for fluorescence lifetime studies, *J Fluoresc*, 14 (2004) 151-71. doi.
- [4] M.C. Gonzalez-Garcia, P. Herrero-Foncubierta, S. Castro, S. Resa, J.M. Alvarez-Pez, D. Miguel, et al., Coupled Excited-State Dynamics in N-Substituted 2-Methoxy-9-Acridones, *Front Chem*, 7 (2019) 129 (1-13). doi: 10.3389/fchem.2019.00129.
- [5] R.L. Teeuwen, S.S. van Berkel, T.H. van Dulmen, S. Schoffelen, S.A. Meeuwissen, H. Zuilhof, et al., "Clickable" elastins: elastin-like polypeptides functionalized with azide or alkyne groups, *Chem Commun*, (2009) 4022-4. doi: 10.1039/b903903a.
- [6] S.H. Choi, K. Kim, J. Lee, Y. Do, D.G. Churchill, X-ray diffraction, DFT, and spectroscopic study of N,N'-difluoroboryl-5-(2-thienyl)dipyrin and fluorescence studies of related dipyrromethanes, dipyrins and BF₂-dipyrins and DFT conformational study of 5-(2-thienyl)dipyrin, *J Chem Crystallogr*, 37 (2007) 315-31. doi: 10.1007/s10870-006-9126-0.
- [7] B.K. Müller, E. Zaychikov, C. Bräuchle, D.C. Lamb, Pulsed Interleaved Excitation, *Biophys J*, 89 (2005) 3508-22. doi.
- [8] J. Schindelin, I. Arganda-Carreras, E. Frise, V. Kaynig, M. Longair, T. Pietzsch, et al., Fiji: an open-source platform for biological-image analysis, *Nat Meth*, 9 (2012) 676-82. doi: <http://www.nature.com/nmeth/journal/v9/n7/abs/nmeth.2019.html - supplementary-information>.

- [9] J. Schindelin, C.T. Rueden, M.C. Hiner, K.W. Eliceiri, The ImageJ ecosystem: An open platform for biomedical image analysis, *Mol Reprod Dev*, 82 (2015) 518-29. doi: 10.1002/mrd.22489.
- [10] M. King, G. Attardi, Human cells lacking mtDNA: repopulation with exogenous mitochondria by complementation, *Science*, 246 (1989) 500-3. doi: 10.1126/science.2814477.
- [11] P. Herrero-Foncubierta, M.d.C. González-García, S. Resa, J.M. Paredes, C. Ripoll, M.D. Girón, et al., Simple and non-charged long-lived fluorescent intracellular organelle trackers, *Dyes and Pigments*, 183 (2020) 108649. doi: <https://doi.org/10.1016/j.dyepig.2020.108649>.
- [12] M.P. Denofrio, F.A.O. Rasse-Suriani, J.M. Paredes, F. Fassetta, L. Crovetto, M.D. Giron, et al., N-Methyl- β -carboline alkaloids: structure-dependent photosensitizing properties and localization in subcellular domains, *Org Biomol Chem*, 18 (2020) 6519-30. doi: 10.1039/D0OB01122C.
- [13] K.W. Dunn, M.M. Kamocka, J.H. McDonald, A practical guide to evaluating colocalization in biological microscopy, *Am J Physiol Cell Physiol*, 300 (2011) C723-C42. doi: 10.1152/ajpcell.00462.2010.
- [14] S. Bolte, F.P. Cordelières, A guided tour into subcellular colocalization analysis in light microscopy, *J Microsc*, 224 (2006) 213-32. doi: 10.1111/j.1365-2818.2006.01706.x.
- [15] A. Orte, E.M. Talavera, A.L. Maçanita, J.C. Orte, J.M. Alvarez-Pez, Three-State 2',7'-Difluorofluorescein Excited-State Proton Transfer Reactions in Moderately Acidic and Very Acidic Media, *J Phys Chem A*, 109 (2005) 8705-18. doi: 10.1021/jp051264g.
- [16] A. Orte, L. Crovetto, E.M. Talavera, N. Boens, J.M. Alvarez-Pez, Absorption and Emission Study of 2',7'-Difluorofluorescein and Its Excited-State Buffer-Mediated Proton Exchange Reactions, *J Phys Chem A*, 109 (2005) 734-47. doi: 10.1021/jp046786v.
- [17] D. Miguel, S.P. Morcillo, A. Martin-Lasanta, N. Fuentes, L. Martinez-Fernandez, I. Corral, et al., Development of a New Dual Polarity and Viscosity Probe Based on the Foldamer Concept, *Org Lett*, 17 (2015) 2844-7. doi: 10.1021/acs.orglett.5b01275.
- [18] M.C. Gonzalez-Garcia, T. Peña-Ruiz, P. Herrero-Foncubierta, D. Miguel, M.D. Giron, R. Salto, et al., Orthogonal cell polarity imaging by multiparametric fluorescence microscopy, *Sens Actuator B-Chem*, 309 (2020) 127770. doi: 10.1016/j.snb.2020.127770.